Technische Universität München
Department of Civil, Geo and
Environmental Engineering
Chair of Cartography

Universidad Politécnica de Valencia
Department of Cartographic Engineering,
Geodesy and Photogrammetry

APPLICATION OF MULTI-TEMPORAL FRAGMENTATION INDICES IN THE CHARACTERISATION OF URBAN DEVELOPMENT

MASTER'S THESIS

Katalin Joó

Submitted: 31.08.2017

Study Course: Cartography M.Sc.

Supervisors: Luis Ángel Ruiz Fernández (UPV)

Marta Sapena Moll (UPV)

Juliane Cron (TUM)

DECLARATION OF AUTHORSHIP

I hereby declare that the submitted master thesis entitled “Application of multi-temporal fragmentation indices in the characterisation of urban development” is my own work and that, to the best of my knowledge, it contains no material previously published, or substantially overlapping with material submitted for the award of any other degree at any institution, except where acknowledgement is made in the text.

Valencia, 31 August 2017 Katalin Joó

ACKNOWLEDGMENTS

Hereby, I would like to take the opportunity to express my gratitude to every professor, classmate and friend who accompanied and supported me in this long academic journey starting from Hungary through Norway, Germany, Austria and finally finishing in Spain.

My deepest gratitude goes to my supervisors Luis Ángel Ruiz and Marta Sapena at Universidad Politécnica de Valencia (UPV) for their constant guidance, availability, ideas and kindness during all these months. I had never expected to receive so much support. Equally, special thanks to Juliane Cron, my supervisor at Technische Universität München (TUM), for her support, patience and valuable feedback on my work.

In addition, the biggest thank you to my family, who has always been there for me.

ABSTRACT

Urbanisation, encouraged by population growth and fast industrial and economic development, is changing the face of the Earth day by day. The newly urbanised areas appear and spread at the cost of the extension and unity of green areas and their ecosystem. To be able to reduce the negative effects of urbanisation, it is important to monitor, analyse and understand urban growth. Many studies have been conducted on the topic to help urban planners realise more sustainable development. This thesis also aims to contribute to a better understanding of urban growth. Fragmentation indices were used in the characterisation of urban development, but not only considering the changes in historical datasets as in other studies but simulated data for the future was also included. For the study area of Valencia historical data was gathered to create land use maps and simulate future scenarios demonstrating the characteristics of isolated, compact, combined and road based growth. These served as the input data for multi-temporal fragmentation analysis with the IndiFrag tool. Based on the calculated metrics, the scenarios were classified into the four growth types. The results of the classification and the original growth types of the scenarios were compared with statistical methods to evaluate the accuracy of the classification based on the metrics. The results show that multi-temporal fragmentation indices can contribute to urban development characterisation by describing the growth type in the area.

LIST OF FIGURES

LIST OF TABLES

ABBREVIATIONS

ABM	Agent Based Model
ANN	Artificial Neuron Network
C	Compact
DTM	Digital Terrain Model
FI	Fragmentation Indices
I	Isolated
IGN	Instituto Geográfico Nacional (National Geographic Institute)
INE	Instituti Nacional de Estadística (National Institute of Statistics)
LU	Land Use
LULC	Land Use Land Cover
MI	Multi-temporal Indices
R	Road-based
SO	Super-Object
U	Urban class
UA	Urban Atlas
X	Combined

TABLE OF CONTENTS

1 INTRODUCTION

1.1 Context and Relevance of the Topic

Urbanization is inevitable due to industrial and economic development and rapid population growth, but cities, especially the suburban regions are also expanding because of the spatial change in population and the shift to low density development in these regions (Shalaby et al., 2004). The tendency of living in suburban areas surrounding big cities and commute on a daily bases gave a boost to the expansion of suburban habitats (Theobald, 2005; Yuan et al., 2005).

According to the United Nations' data, the total population of the world in the last 64 years has almost tripled (data until 2014), and surpassed 7 billion by 2014. Not only the population is increasing constantly, but many people find the potentials offered by cities attractive, such as more and better paying job opportunities, better infrastructure, better health service and access to other social benefits and services. In the hope of better living standards people leave the rural areas for the city. In 1950 only less than 30 percent of the population lived in urban areas, while by 2014 more than half of the population of the world lived in cities and the tendency does not seem to stop (UN, 2017).

Urban land accounts for only a small portion of the Earth's surface. Still, urbanization is a critical factor in land use change converting green areas into residential, industrial and commercial use (Fang et al., 2005; Luck and Wu, 2002). The shift to suburban areas form city centres leads to low density development of large areas of land scattered around big cities, for single use. This results in a large urban footprint even without high increase in population (Theobald, 2005). Rapid population growth and unplanned urbanization bring risks of pollution, increase of traffic, deforestation, overpopulation, climate change, loss of biodiversity and fragmentation of non-urban habitats (Foley et al., 2005; Hannah, 2011).

The abundance of already existing literature written about urbanization, urban sprawl, monitoring cities, urban growth modelling and land use land cover change demonstrates the importance of the phenomenon. Scientist and experts have been monitoring the development of cities and the changes in land use cover in order to simulate spatiotemporal patterns of urban growth with the help of which, future growth of cities and the changes in land use can be predicted (Weber, 2003). The importance of an accurate and updated database of land cover change is to be able to understand and evaluate the environmental consequences, as well as to improve decision making when it comes to designing sustainable urban habitats (Arsanjani et al., 2013).

1.2 Problem Definition and Motivation

The most intricate land use change is urban sprawl due to the number and complexity of its driving forces, their own processes and their interactions and influence on each other. These drivers that define the rate and spatial expansion of urban growth are economical, physical, political and environmental (Ligtenberg et al., 2001). Various methods have been developed in order to describe and simulate the dynamics of urban sprawl, each model considering different factors. However, because of the complexity of the system it is difficult to capture all the drivers at once and to find the appropriate weight for each when combining them (Fang et al., 2005). These urban sprawl simulating models are among others agent based models, cellular automata, fractals, neural networks, regression models, decision trees and their combinations (Triantakonstantis and Mountrakis, 2012).

One side effect of urbanisation and other human activities, such as deforestation and agriculture, is the fragmentation of the landscape which has been examined and described by several studies (Kamusoko and Aniya, 2007; Nagendra et al., 2004). On the one hand, fragmentation can be observed in a global level of the landscape to monitor deforestation and the fragmentation of habitats. However, on the other hand, it can be examined within the urbanised areas as well, to help the understanding and interpretation of the structure and characteristics of the cities (Linh et al., 2012; Yin et al., 2010). The fragmentation of the landscape is measured by metrics that describe features, such as area, perimeter and average size of the objects, while the changes in the fragmentation are examined by multi-temporal indices or the comparison of

temporal metrics (Liu et al., 2010; Sapena and Ruiz, 2015a). It is important to monitor and simulate urban development so that urban planners can work on more sustainable form of urbanisation. Multi-temporal fragmentation metrics can be a useful tool for them to analyse urban sprawl and the changes within the urban area. It is interesting to see whether the metrics can give useful information about the growth type of the urban area.

1.3 Research Objective and Research Question

The objective of the thesis is to determine the applicability of multi-temporal fragmentation indices to urban development characterization. In order to accomplish this, Land Use and Land Cover (LULC) maps from previous years need to be collected and predicted LULC maps need to be created. The fragmentation indices are applied to these past and predicted LULC data using the IndiFrag tool (the tool is described in Chapter 3.6). The resulting metrics are then examined with the help of statistical analyses in order to answer the research question: Can multi-temporal fragmentation metrics contribute to the characterisation of urban development?

1.4 Outline of the Thesis

The thesis is organized into five main sections. Following the introduction, Chapter 2 is a brief overview of the available literature on land use modelling and simulation from which a suitable model had to be selected for the case study. Chapter 3 discusses the methodology of the thesis starting from the study area, data sources and preparation, then describing the preparation of the scenarios and the application of the fragmentation metrics on them and finally the analyses conducted on the metrics were introduced. The results of the analyses are presented and explained in Chapter 4, which is followed by the conclusion focusing on the interpretation and importance of the outcomes and possible future research on the subject.

2 LITERATURE OVERVIEW

This chapter gives an overview of the available models used for urban growth modelling. The short descriptions introduce the methods in order to be able to select the most appropriate one for the current study. There already exist a wide variety of methods to predict urban growth and land use change. A retrospective summary of existing literature on urban growth prediction models was created by Triantakonstantis and Mountrakis in 2012 identifying more than 1400 records. After removing unrelated records, models not spatially explicit, manuscripts with only theoretical component and applications of previously published work, the remaining 156 studies were included in a qualitative synthesis. The articles introduced seven different types of urban growth prediction models as follows: 1) Cellular Automata (CA), 2) Logistic Regression, 3) Artificial Neural Networks (ANN), 4) Fractals, 5) Agent Based Models (ABM), 6) Linear Regression and 7) Decision Trees. Cellular Automata stands out significantly among the algorithms in respect of popularity as it is included in more than 80 % of the analysed papers. The models work with different methods and incorporate different driving factors such as environmental, social and economic. In the following paragraphs the most widely used models (1-5) are briefly introduced to get an overview of the currently available options for urban growth modelling.

The concept of **Cellular Automata (1)** was discovered by Stanislaw Ulam and John von Neumann in the 1940s. Four decades later Wolfram (1984) used CA to describe the nature and generation of complex systems whose complexity was generated by fundamental components that are very simple. The first applications of the technique to geographic modelling also appeared in the 1980s using artificial cases to develop theoretical models, which finally led to the first operational urban CA models applied to real-world urban system in the 1990s (Santé et al., 2010). The basic unit in the model is the cell. The discrete space is divided into regular cells. Each of them has a state which can change by following predefined transition rules that consider the state of the cell

and its neighbourhood (the cells adjacent or close to the cell in particular). The interactions occur on a local level at each time step in the discrete time, and the combined actions of these local transitions conclude the overall performance of the system (Arsanjani et al., 2013). These are the characteristics of the conventional CA where the model can be adopted to the selected study area by different transition rules. However, by modifying the structures of the standard CA the model can be used to describe more complex geographical phenomena: introducing irregular, non-uniform cell space; extended, non-stationary neighbourhood; more complex, non-stationary transition rules, growth constants and irregular time steps (Couclelis, 1985, 1997; Santé et al., 2010).

An already widely used CA model is the **SLEUTH model**, written in the C programming language. The first article was published in 1997 introducing the model with a case study on the San Francisco Bay area (Clarke et al., 1997). Ever since then several reviews have been written and case studies have been conducted all over the world proving, challenging and improving the use of the method (Clarke and Gaydos, 1998; Dietzel and Clarke, 2007; Silva and Clarke, 2002; Terando et al., 2014, etc.). According to (Chaudhuri and Clarke, 2013) SLEUTH has been successfully applied in 18 countries in the world to more than 35 regions until 2012. The model aims to predict scenarios of future land transformation based on several different types of historical data, such as transportation network, topography, existing urban distribution, land use coverage and restricted areas. The data are gathered from more than one time period, which makes the calibration possible by monitoring the modifications over time. The model works with raster data, more specifically with grayscale GIF images. Based on the historical data, the five coefficients the model works with are calibrated in three steps: coarse, fine and final calibration or manually by the user. The five variables are the diffusion, breed, spread, slope and road gravity. After each calibration the user sets the value range for each coefficient more and more precisely based on the result of the previous calibration. The model works with four types of urban growth rules that are controlled by the coefficients: spontaneous growth, new spreading centres, edge growth and road influenced growth. The uncertainty is included in the model with the help of Monte Carlo iterations, which is an algorithm that rely on repeated random sampling to obtain numerical results such as the distribution of an unknown probabilistic entity

(Hussain and Ivanović, 2015). Control parameters let the system modify itself and this way adopts to periods of high and low growth in urbanisation. The output images are the same format and size as the input layers. Besides predicting the urban extent or land use cover for each year until the selected year, there are other output options as well: images showing the urbanised areas according to which type of growth rule occurred and statistical data.

The **Logistic Regression Model (2)** developed by Cox (1958) is an empirical estimation model used in statistics. A commonly used logit regression model in urban change modelling is the binary, which calculates the probability for an observation (the dependent variable) to be 0 or 1 based on one or more categorical or continuous independent variables. It was applied in urban growth prediction for example by Hu and Lu (2007). They considered demographic, economic and biophysical driving forces as categorical and continuous independent variables to define whether a cell is urbanised or not, assuming that the logistic curve of the logistic function gives the probability of urbanisation in a cell. Multivariate logit regression models can also be applied to urban sprawl monitoring (Alsharif and Pradhan, 2013), as this statistical method is useful in analysing the relation of the driving forces to urbanisation. It helps to select the most important variables in urban sprawl monitoring (Allen and Lu, 2003; Park et al., 2011). It is often integrated with other urban simulation methods, such as cellular automata (Arsanjani et al., 2013).

Artificial Neural Networks (3) are powerful computing systems in the recognition of complex patterns in data due to their ability to learn by trial and error method (Tayyebi et al., 2011). The model is inspired by the brain of animals, which can process multiple signals, and has been used in a great variety of scientific fields for pattern recognition: economics, medicine, mechanical engineering, landscape recognition and remote sensing (Pijanowski et al., 2002). An advantage of the model in urban growth simulation is that it is capable of solving highly nonlinear problems which are common in the complex phenomena of urbanisation. The basic units of the network are the neurons. They are arranged in layers where they work in parallel. The neurons are connected only to the neurons of the next layer (neither to other layers, nor neurons form the same layer) (Maithani, 2009). The weights that define the output are carried in the connections between the neurons. In multilayer perceptron, between the input and

output layers there is one (or more) hidden layer(s), which processes the weighted data received from the input layer and forwards it for further processing to the output layer. The input neurons represent the input data sources, the neurons of the hidden layers have to be calculated and the output neurons stand for the classes being mapped (Kanungo et al., 2006). A commonly used learning procedure is the back-propagation introduced by Rumelhart et al. (1986), where a training set is introduced to the model as the input layer and using random weights the output is calculated. Then the calculated output is compared to the expected output and to eliminate the error, the weights are adjusted. It is repeated until the results are adequate. The training results are tried on a testing dataset as well to evaluate the performance.

Fractal modelling (4) gained popularity in various sciences after the publication of Mandelbrot (1983), which is a revised and extended version of the writer's previous works. He named 'fractal' the shape that can describe irregular forms and rough surfaces, something that the previously used Euclidean geometry was not able to. From the 80s it was applied to describe urban structure and development as well (Batty and Longley, 1986, 1987; Fotheringham et al., 1989) since the irregularity and scale independence of urbanisation shows the characteristics of fractals (Shen, 2002). The ability of the fractals to give more detail at every scale level is due to the generator rule. The initial shape is given by a Euclidian figure called initiator and the generator transforms the evolving figure at each iteration following self-similarity rules (Mandelbrot, 1983). For example some simple self-similarity rules from Frankhauser (2008):

"1. The size of the initiator, e.g. a square, is reduced by a certain factor r

2. N of these little replicates are generated

3. These N replicates are placed in a defined way, respecting the following restrictions: they must be placed within space occupied by the initial figure, i.e. they must be subsets of the initiator; they are not allowed to intersect."

Frankhauser also explains that the number of possible iterations is endless. Usually the procedure is stopped when the size of the elements correspond to that of a building. The elements that make up the fractal can be detached or interconnected. One example of a fractal consisting of unconnected elements is the so called Fournier dust, while in the

Sierpinski carpet the elements are interconnected and this way form a single cluster (Tannier et al., 2011). The initial form does not have to be two dimensional it can also be a line segment showing the boundary of urban areas. This fractal is called teragon. As the urban pattern does not follow a symmetrical order random fractals can resemble them more accurately. Certain parameters of the fractals can be calculated for the urbanised areas and used for the characterisation of urban pattern, for example fractal dimension and fractal order. The majority of the literature on fractals describing urbanisation aims to define the form, structure and features of urban patterns and characterise urban growth and morphology. On the other hand, for example Triantakonstantis (2012) used the Sierpinski carpet to find the most suitable areas for urban development.

Agent Based Models (5) bring the impact of human behaviour in urban growth simulation with the help of agents governing urban growth (Zhang et al., 2010). The agents can represent several environmental, social and economic features. Arsanjani et al. (2013) introduced three agents: resident, developer and government, behaving as the main actors of land use change in each pixel. Resident agents are the people relocating in the city from elsewhere or locals relocating within the city. Their preferences are mostly influenced by environmental and socio-economic driving forces, such as the steepness of the landscape and accessibility to transportation. A probability surface was created based on a multi-criteria analysis that presents the cells suitable for development according to the residents. Housing companies belong to the developer agents, who facilitate the construction for urbanisation. Their decisions are guided by the maximum profit, which can be reached considering the need of the potential residents and the government policies. In the probability surface of developers the investment profit is calculated for each pixel based on housing, land prices and development cost. The government agent represents the restrictions introduced by policy makers. They prohibit the urbanisation of certain areas, for example parks, water, certain buffer zone along transportation networks etc. These were converted into a Boolean image where the cells are either allowed or not to be urbanised. Later the actual simulation of growth is simulated with the help of Markov chain and CA model. The three agents represent individual decisions influenced by biophysical, social and economic factors and together result in a collective outcome. The model can work with different agents

representing different urban growth drivers. For example Zhang et al. (2010) work with a similar concept of three agents too, but besides resident and government agents instead of the developer agents they considered peasants. They represent an important part of the population in China, who lives from agriculture and wants to stay close to their land but also close to the city. Magliocca et al. (2012) examines the interaction between developer, costumer and landowner who decides whether or not to sell their parcel.

Markov chain is a stochastic progression that has been used in urban growth modelling combined with other approaches as a supplement (Arsanjani 2013). It calculates the probability of change between states. The two tables generated by the model (transition probability matrix and transition area matrix) determine the amount of change between the classes. However, since the exact spatial location for the change is not considered, a further method is required to localise the change. Arsanjani, (2011) used a CA, for example.

Beside the Markov chain other models can also be combined with each other to integrate their advantages and complete each other. ANN is commonly used together with CA (Yang et al., (2015); Li and Yeh, (2010)), where ANN functions as the data mining tool to find the transition rules and the CA provides the framework for the spatio-temporal changes in the landscape. Tian at al. (2016) combined CA with agents and logistic regression. The human system was represented by two agents. The authority agent determines the location priorities of urban development and the resident agent represents the urban residential location decisions. The landscape is described by a two dimensional cellular space, where each cell has its coordinates and an attribute referring to the land use type. The changes of the dynamic landscape system are driven by biophysical driving factors following the rules of cell transition. Logistic regression was used to calculate the probability of urban expansion by self-organisation of the landscape system.

The overview of the urban growth simulating methods has importance in the selection of a model for the scenario simulations. After the introduction to the most commonly used models, it is clear that although, each of them computes possible future scenarios they are all slightly different, which can lead to very different outcomes. This

diversity is due to the complexity of urban growth and land use change and it provides more options to choose from when selecting a model for urban growth analysis. Their main differences lay in the necessary input data, the type of output, the applied urban growth drivers, the required computational power and how much control the user have over the settings. These were considered in the selection of the model described in Chapter 3.4.

3 METHODOLOGY

The third chapter starts with the declaration of the research approach and the introduction to the growth types to be examined andto the selected study area. Then, the complete workflow of creating the scenarios for the fragmentation analysis with the SLEUTH model is explained, followed by the description of the fragmentation analysis with the IndiFrag tool. Finally, the methodology of the classification and the validation is outlined before revealing the results in the next chapter.

3.1 Research approach

The research objective was examined with the help of a case study conducted on Valencia. A database of simulated scenarios was created on the study area with the help of an urban growth prediction model to analyse the use of multi-temporal fragmentation metrics in the characterisation of urban growth. The results were computed and evaluated with the help of statistical analyses using the statistical software STATGRAPHICS.

3.2 Growth types

The urban development in the study area was characterised by examining the type of growth occurring in the area. Wilson et al. (2003) and Camagni et al. (2002) distinguished five different urban expansion types in a similar way. Wilson et al. identified three main types: infill, expansion and outlying that was further divided into three more growth (isolated, linear branch and cluster branch). Camagni et al. used different names for the growth types but followed the same division: infilling, extension, sprawl, linear development and large-scale projects. They additionally also identified the combinations of these expansion types and selected the five most prevalent from the combinations of two main growth types: linear / sprawl, extension / sprawl, extension / linear, infilling / sprawl and infilling / extension. Yue et al., (2013)

used the three main growth types in their study: infilling, edge-expansion and leapfrog development and Sun et al. (2013) also followed the same division as suggested by Wilson: infilling, edge-expansion and outlying. Table 3.1 summarises the different categorisations.

<table>
<tr><th colspan="2">Wilson et al.</th><th>Camagni et al.</th><th>Yue et al.</th><th>Sun et al.</th><th>This study</th></tr>
<tr><td colspan="2">infill</td><td>infilling</td><td>infilling</td><td>infilling</td><td rowspan="2">compact</td></tr>
<tr><td colspan="2">expansion</td><td>extension</td><td>edge-expansion</td><td>edge-expansion</td></tr>
<tr><td rowspan="3">outlying</td><td>isolated</td><td>sprawl</td><td rowspan="3">leapfrog development</td><td rowspan="3">outlying</td><td rowspan="2">isolated</td></tr>
<tr><td>cluster branch</td><td>large-scale projects</td></tr>
<tr><td>linear branch</td><td>linear development</td><td>road-based</td></tr>
<tr><td></td><td></td><td>combinations</td><td></td><td></td><td>combined</td></tr>
</table>

Table 3.1 Comparison of the growth types in the current and other studies

In this study the infilling and extension growth was combined into **compact growth**, since they similarly occur near already existing urban areas, as opposed to the outlying growth, which develops separately from the existing centres. The outlying growth was named **isolated.** From the three outlying subclasses of growth only to the linear branch was given significance. It was introduced **as road based growth**, because it appears near the linear line of the transportation systems. Following the combination of growth types by Camagni et al. (2002) a **combined growth** was introduced by joining the compact and isolated growth.

In the analysis of the development of the city not always all four types of growth were examined. Three cases were introduced based on the growth types considered in the analysis. Case 1 discriminates two types: isolated and compact; Case 2 three types: isolated, compact and combined; while Case 3 four types of growth: isolated, compact, combined and road based.

3.3 Study Area

The study was conducted on the metropolitan area of Valencia, Spain, located on the eastern side of the Iberian Peninsula, on the cost of the Mediterranean see. The

centre of the study area is located at a latitude and longitude of 39°27'44.5" and 0°23'0.3", respectively. It is based on the alluvial plain of the Júcar and Turia rivers, as a result of which the area is quite flat (Piqueras Haba, 1999). This makes the urbanisation of the city relatively easy without the limitations of high mountain areas. The lake of Albufera and the national park surrounding it prevent the city from growing on the south along the cost (Figure 3.1, District 16).

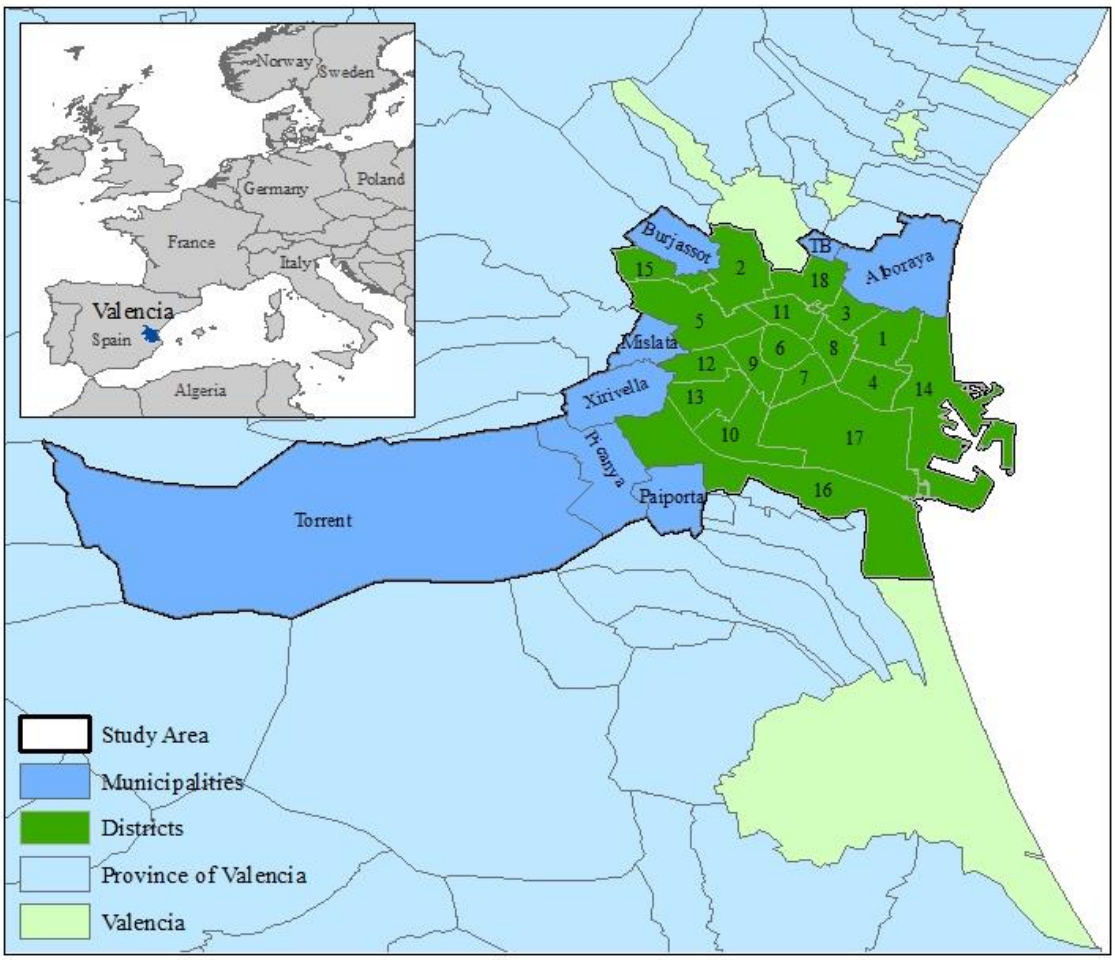

Figure 3.1 Study Area of Valencia (Data: INE (2017))

According to the National Statistics Institute it is third among the most populated cities in Spain after Madrid and Barcelona, holding at present a total population of 790 201 (INE, 2016). The metropolitan area was previously called the county of Huerta. Today it consists of the city of Valencia and three other counties on the northern, southern and western side of the city named Huerta Norte, Huerta Sur, Huerta Oeste respectively. The city of Valencia is divided into 19 districts, and the three

counties consist of 44 municipalities surrounding the city. Administratively they belong to the capital province of the Valencian Community (INE, 2017).

For the purpose of the study the areas showing strong residential growth in the last 20 years were selected, as the aim was to monitor and analyse these changes and use this information to simulate future scenarios. The study area covers an approximate area of 185 square kilometres, which includes 18 districts of the city and 8 municipalities on its northern and western side (Figure 3.1). The national park of Albufera in the district of Pobles del Sud (District 16) was not considered, because it is a protected area with no changes in land use. The terrain mainly features plains and a few hills in the western corner of the municipality of Torrent. The average slope is less than 3 degrees (CNIG, 2017).

3.4 The selected model for the study

For the characterisation of urban development an urban growth model had to be selected. The scenarios of the four growth types were created using environmental driving forces. In the scenarios not only urban growth was simulated, but also land use changes were to be detected. As a result, it was important that the model can not only predict urban change, but is able to incorporate more than one land use type in the simulation, such as CA and ANNs. Moreover, to be able to examine the accuracy of urban development characterisation by fragmentation metrics, it was necessary to understand and be able to control the transition rules of the simulation. One disadvantage of ANNs is that the calculations are not visible to the user and has no control over them (Maithani, 2009). The CA also works with a trial and error method like the ANN, but the transition rules can be modified by the user, as a result the rules are transparent (Arsanjani at al., 2013). From the models introduced in Chapter 2, CA proved to be the most suitable for this study since it meets all the most important requirements for the simulation. The operation of CA models are computation intensive (Hu and Lo, 2007), but since the study was conducted on a relatively small area the computation time was not extremely high.

A huge advantage of the selected SLEUTH model is that it is freely available at the Project Gigalopolis website with a short introduction to the model and explanation

of the use form downloading through calibration and prediction until interpretation of the results (Project Gigalopolis, 2017). As an illustration a demo city was created with the help of which the model's structure and functions can easily be understood. There is a forum for further discussions in case of questions or problems.

3.5 Application of the SLEUTH model

This chapter describes the creation of the scenarios with the SLUTH model from the raw input data to the simulated scenarios ready for the fragmentation analysis. Besides, the operation of the model is explained briefly for better understanding of the procedure.

3.5.1 Input requirements and data description

In the SLEUTH model the future changes in land use are predicted based on the tendencies of previous land use change. The model is named after the abbreviation of the first letters of its six input data types: Slope, Land use, Excluded, Urban extent, Transportation and Hill shade. These are essential to compute the calibration and prediction of data. These data were gathered for the study area of Valencia from three sources (Table 3.2): Urban Atlas by Copernicus (Copernicus, 2017), Digital Terrain Model provided by Instituto Geográfico Nacional (IGN) (CNIG, 2017) and cadaster maps supplied by the Dirección General del Catastro (Sede Electrónica del Catastro , 2017). The administrative boundaries for excluding the areas outside of the study area were provided by the Instituto Nacional de Estadística (INE, 2017).

SOURCE	PROVIDER	YEAR	INPUT
URBAN ATLAS	Copernicus	2006	land use
			road
		2012	land use
			road
			excluded
CADASTER	Dirección General del Catastro	1994	urban
		2000	urban
		2006	urban
		2012	urban
DTM	Instituti Nacional de Estadística		slope
			hillshade

Table 3.2 Data sources for the input layers

The model requires at least two land cover layers from different years as **land use** input, from which the last year has to correspond to that of the urban extent. Two options were considered: Urban Atlas data for 2006 and 2012 and the Official cartography of the Valencian Community supplied by ICV (Instituto Cartográfico Valenciano) for the years 2000 and 2008. The later source has differences in reference datum and scale between the two years. In order to be able to compare the changes that occurred between the two dates in land use cover, the datum and scale need to be transformed to be the same. This transformation can lead to differences in the x, y values and cause changes in land use cover that did not occur in reality. This proved the Urban Atlas data to be more reliable in regards of comparison. In the Urban Atlas there are also small differences between the land use maps of the two years, but only in the categorization of land use types. Table 3.3 demonstrates the categories or decision rules of the 2012 version with its five main categories: artificial surfaces, agricultural, natural and semi-natural areas, wetlands and water. In the 2006 version, agricultural land use is in the same group with semi-natural areas and wetlands, while forests have a separate category. This did not influence further calculations with the two databases. The artificial surfaces are divided into several more classes and sub-classes. Table 3.3 shows which Urban Atlas land use classes were merged to create the four land use types of this study: urban, agricultural, road and green area and the excluded mask.

It is important to include **transportation** in the predication to see how much influence they have on urban development in the particular area. Transportation networks provide accessibility, for this reason urban development has a tendency of demonstrating higher growth near road network centres. At least data from two years are needed to see how the transportation changes with urban development. The first road layer is used for initialisation and the next ones are read in when their year is reached as growth cycles pass. The road networks were retrieved form the Urban Atlas as well the same way as before. As a result the two input dates are the same as in case of the land use (2006, 2012).

URBAN ATLAS			
	1. Artificial surfaces	1.1 Urban Fabric	1.1.1 Continuous urban fabric
			1.1.2 Discontinuous dense urban fabric
			1.1.3 Isolated structures
		1.2 Industrial, commercial, public, military, private and transport units	1.2.1 Industrial, commercial, public, military, private units
			1.2.2 Road and rail network and associated land
			1.2.3 Port areas
			1.2.4 Airports
		1.3 Mine, dump and construction sites	
		1.4 Artificial non-agricultural vegetated areas	1.4.1 Green urban areas
			1.4.2 Sports and leisure facilities
	2. Agricultural		
	3. Natural and semi-natural areas	3.1 Forests	
		3.2 Herbaceous vegetation association	
		3.3 Open spaces with little or no vegetation	
	4. Wetlands		
	5. Water		

URBAN
AGRICULTURAL
GREEN AREA
ROAD
EXCLUDED

Table 3.3 Urban Atlas classes divided into land use and excluded layers

The **slope** layer demonstrates the elevation of the area, which is an important factor in urbanisation, since the steeper and higher the hills are, the more difficult it is to construct upon them. The Digital Terrain Model was supplied by the Instituto Geográfico Nacional (IGN). MDT05 is a digital elevation model with 5 meter resolution in the Geodetic Reference System ETRS89 and its corresponding UTM projections. The data are obtained by the PNOA (National Aerial Orthophotography Plan) by either the correlation of photographic flights with 25 or 50 cm pixel size or by interpolation of LIDAR flights (Centro de Descargas del CNIG, 2017). The cartographic grids covering the study area are 696, 721 and 722. These were merged to get the total coverage of the area. From this digital elevation model the slopes were calculated in percentage**. Hill shades** were also retrieved from the same DEM serving as the background for the urban extent prediction to give spatial context. The topological information is obtained from the slope layer. The hill shades only help spatial orientation. It is only used for urban extent as the land use classes cover the whole area.

The input layers of **urban** extent show the changes in urbanisation, for this reason images from several years are needed. The earliest urban extent layer is the so called seed, from where the calibration starts. Urban extent layers from at least three more years are needed for the calibration, used to calculate best fit values. The Urban Atlas could not be used as source for the urban layers since it provided data for only two years. The cadastre maps of the Dirección General del Catastro provided sufficient data for four years: 1994, 2000, 2006 and 2012. The time period that the historical data covers can be chosen by the user depending on data availability or of interest. The four years were chosen following the time slots of six years in the Urban Atlas and later years could not be selected since the most recent year has to agree to that of the land use layers. The cadastral information can be downloaded by municipality with permission from the directorate. The urban cover was obtained from the fields marked as rural areas selecting urban plots and constructions. The plots were distributed in the four urban masks based on the cadastre attribute files, which contain the earliest date the plots appear in the database.

The model allows **excluding** areas that have high resistance to urbanisation. For example water surface, wetland or protected areas. In this study additionally the river park Turia, the river bed of the river Turia, roads, a cemetery and the port area were excluded due to low probability of being urbanised in the near future. The selection of areas was based on the Urban Atlas data (Table 3.3). The surrounding area was also excluded because it is not considered in the current study. The administrative units from INE were used to select the 18 districts and 8 municipalities and cut the surrounding areas.

3.5.2 Preparation of Input for the SLEUTH model

After having collected all the necessary input data, further processing was conducted with the help of the geographical information system ArcGIS. Figure 3.2 shows the work flow of converting the raw data into the input data. The first step was to eliminate the parts outside of the study area. The administrative boundaries provided by the Instituto Nacional de Estadistica (INE) were used to cut the areas surrounding the selected municipalities.

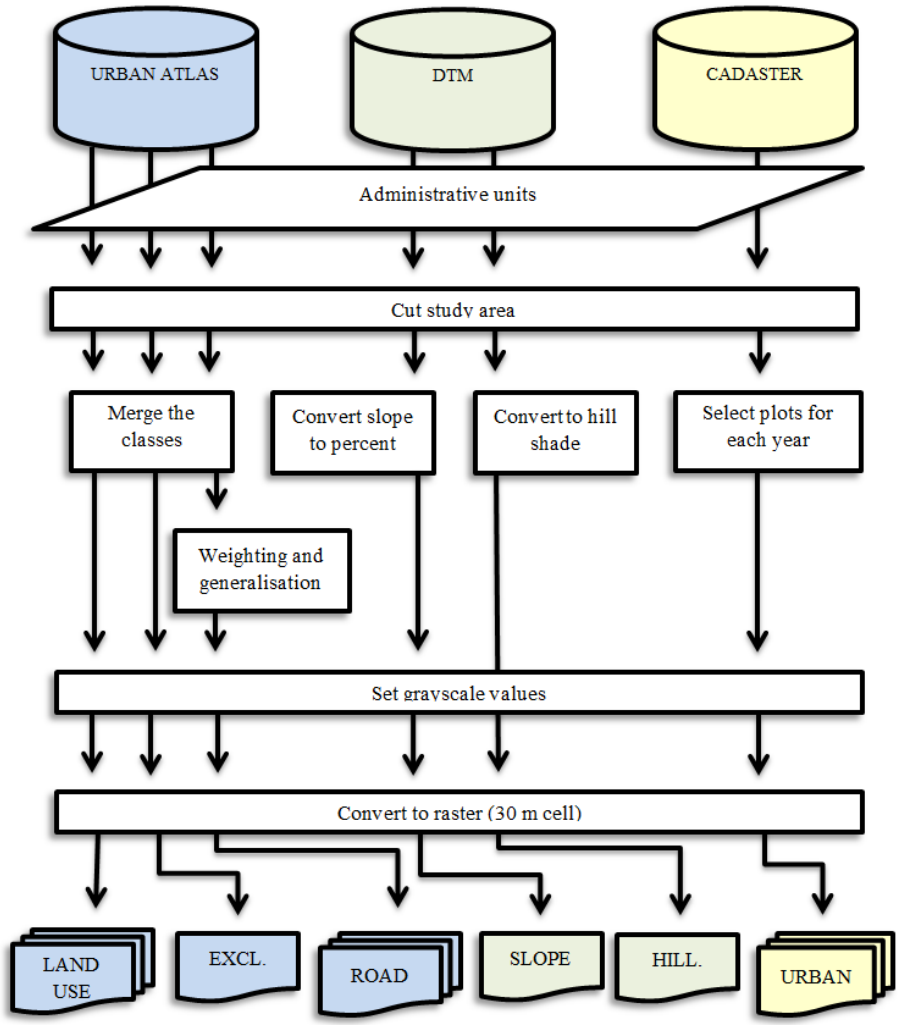

Figure 3.2 The work flow from raw data to the input data

The model differentiates between the classes within the layers with the help of differences in grayscale values. In all the layers 0 is a null value and integers greater than 0 and smaller than 255 are existing values. In binary layers such as urban extent and transportation, the pixels with value of 0 stand for non-urban/no road areas. Any other value means that the area is urbanised/with transportation. In the excluded mask the area can be divided into three levels of resistance: available for development (indicated by value of 0), low resistance for development (indicated by a value between 0 and 100) and high resistance or development is impossible (indicated by a value of 100 or greater). The excluded areas were all marked with high resistant to prevent any possible urbanisation in the simulation. The slopes are not given in degrees, but in percentage. This means that the pixel values range from 0 till 100, each representing a

slope percentage. When the slopes surpassed the 100 percentage, they were converted to the max value of 100. In case of the land use masks, to each grayscale value a class of land use is added, so that the model can differentiate between the types. In order to visualise the classes for the user, in the output images for each class an RGB colour value is set. The four urban use classes were marked from one to four in grayscale: 1 – urban, 2 – agricultural, 3 – road and 4 – green area.

The input file format is raster. All the images are required to have the same map extent and cell size, which means equal number of rows and columns, over the same area, in the same projection and coordinate system so that the model can examine the changes between the data. The coordinate system used for the input layers was the European Terrestrial Reference System 1989 (UTM Zone 30N) in Transverse Mercator projection. The cell size was determined based on trials and examples from previous applications of CA models. In the review of Santé (2010) the cell space ranges between 10 m and 1 km, depending on data availability and whether the studies are conducted on local or regional level. The chosen cell size was 30 m, because the changes simulated at this scale were realistic enough for the study. This results in an image size of 911 x 516 pixels, which is small enough to be able to conduct the calibration steps within a reasonable time period. The size of the pixel affected the display of the roads (both the road and land use masks). The road network in the Urban Atlas is very detailed, including small streets and pavement as well. The isolated pixels of the road class in the land use layers were removed by applying a majority filter sized 3x3 and were replaced by the most frequent land use type in the neighbourhood. In case of the road data, to keep only the main roads, a series of negative and positive buffers were applied. The roads that did not reach the width of six meters were eliminated and to the rest generalisation was applied, because otherwise they would not be visible due to their small size. The vector layers were converted to raster by applying the maximum area criteria. The input images have to follow a predefined naming format given in the scenario file, otherwise the model does not recognise them. Figure 3.3 gives an example of all six input layers. It is important to note that the images are for illustration, not in the original above described grayscale colours.

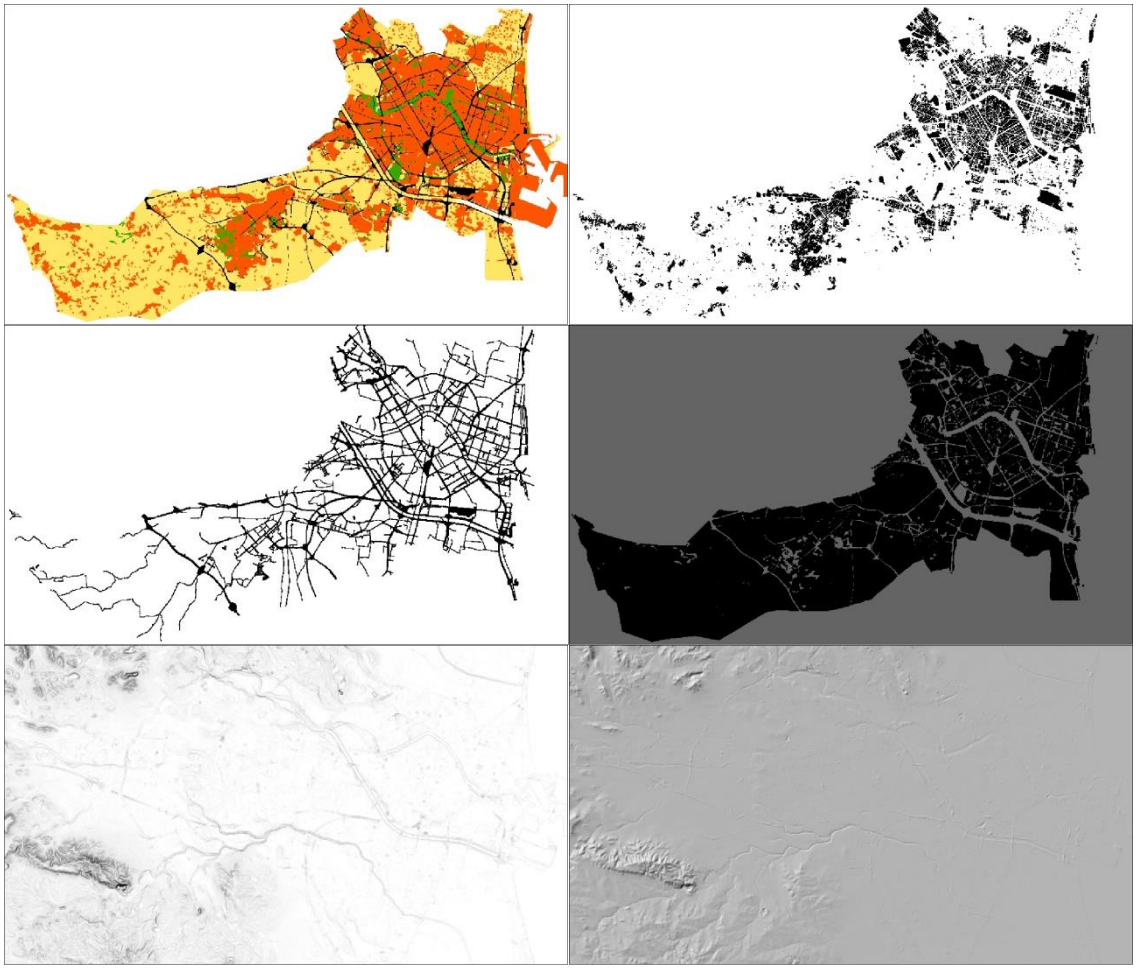

Figure 3.3 Examples of the six input layers for SLEUTH **(a)** land use 2012, **(b)** urban 2012, **(c)** road 2012, **(d)** excluded, **(e)** slope, **(f)** hill shade (images not in the grayscale values used for the model)

3.5.3 The rules of the SLEUTH model

Once all the inputs are ready the calibration and the prediction can start with the help of the scenario file. The variables and settings are adjusted in this file: path names, file names, coefficients, output settings, etc. The program runs in Linux and the most important commands are provided in the Project Gigalopolis website (Project Gigalopolis, 2017). An example scenario can be found in Appendix 1. In order to be able to conduct simulations with the SLEUTH model it is important to understand how it works. The following five sections explain how the model works, starting with the growth cycle, which is the basic unit of the urban growth simulation. Then, the three steps of this cycle are described and finally the land use change simulation is

characterised. The below described information is based on the website, Clarke (1997) and Clarke and Gaydos (1998).

1) The growth cycle

The growth cycle is the basic unit of the SLEUTH execution. It has three steps: in the first one the five growth coefficient values are set. These values control the four growth rules that are applied in the next step. In the final self-modification step the parameters are slightly modified according to the growth rate presented in the cycle. If it is higher or lower than a previously set value (values of “critical high” and “critical low”), the parameters are increased or reduced respectively. One cycle represents the urban growth of one year between the chosen start and stop date. After all the three steps have been executed the model starts the new growth cycle of the following year with the updated urban input layer and modified coefficients. Figure 3.4 shows the three steps of the growth cycle and four steps of the growth rules determined by the five growth coefficients. In the following sections the components of the growth cycle is explained in more detail: growth rules and coefficients, the self-modification rules and the deltatrons.

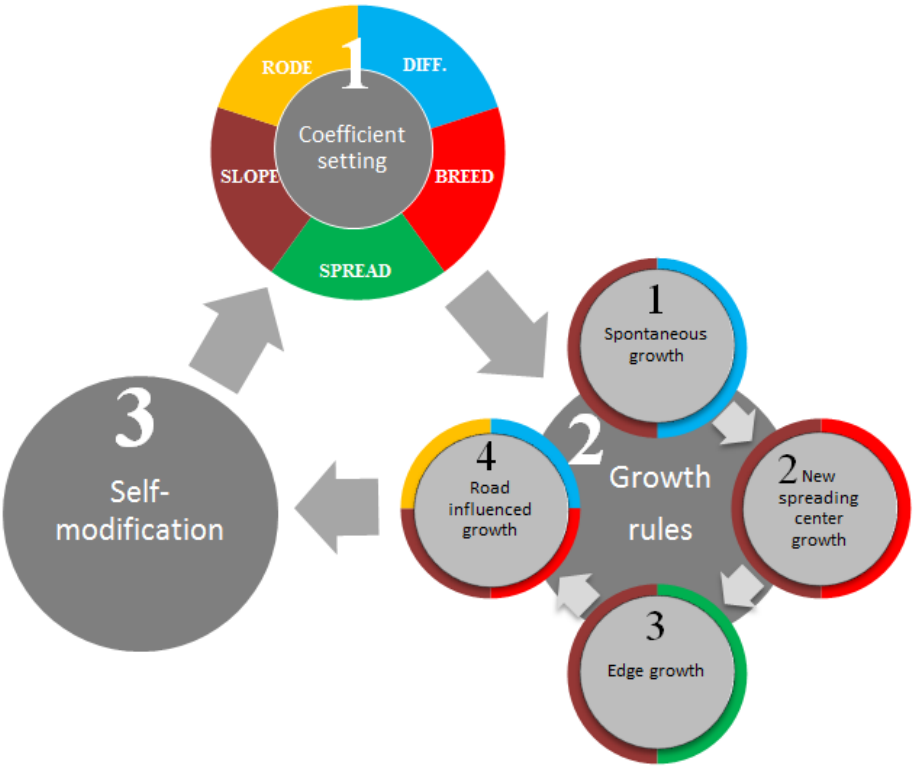

Figure 3.4 The three step growth cycle in SLEUTH: growth coefficients and the growth rules that are controlled by the coefficients

2) Growth Rules

The four growth rules of the SLEUTH model simulate the urban change driven land cover change by randomly selecting the cells suitable for urbanisation and calculating their probability to become urbanised. They belong to the second step of the three step growth cycle and are controlled by the five growth parameters.

Spontaneous growth selects pixels randomly and examines their availability for urbanisation. Available means that they are not yet urbanised, not excluded and their slope percentage is suitable. If all the criteria are met urbanisation will occur in this cell. This growth rule assures that any not yet urbanised pixel can be urbanised at any time step with the probability set by the diffusion coefficient.

The second step is called the **new spreading centre growth**. In this phase the newly urbanised cells are examined, more exactly the pixels in their neighbourhood, to see if they can become a new spreading centres (minimum three neighbouring urbanised cells). If at least two cells are available in this 9x9 square surrounding the selected pixel,

it has the probability defined by the breed coefficient to become urbanised as well. If the cell is found to be suitable to become a new spreading centre two cells next to it will be urbanised.

These spreading centers are important because the third step, the **edge growth** can only occur adjacent to these new centers or already existing centers, but not around single urbanised cells. The spread coefficient determines the probability of urbanisation in this step. In this case the criterion, besides the pixel not being urbanised, neither excluded and nor too steep, is that there has to be at least three adjacent urbanised cells around the selected non-urbanised cell.

The **road-influenced growth** is the most complex from the four rules. It has four steps itself and is controlled by four of the growth coefficients. Urbanisation tends to be higher near transportation networks, and this growth type aims to realise this tendency in the model. The recently (in this cycle or year) urbanised cells are selected with the probability defined by the breed coefficient, and a road is searched in their neighbourhoods within the radius determined by the road gravity coefficient. From this cell a so called “random walk“ is conducted on the road, where the maximum number of steps is determined by the diffusion coefficient. When a cell is finally urbanised, if there are neighbouring cells also available for urbanisation on the road, one or two of them will also be urbanised randomly picked from the available cells.

3) Growth Coefficients

The growth rules are controlled by the five growth coefficients: diffusion, breed, spread, slope and road gravity. All of them have a value range of 1 to 100. They are calibrated based on the historical input data by analysing the changes throughout the years or can be set manually. Each of them has different characteristics and influence on the growth rules:

The **diffusion coefficient** (also referred to as dispersion coefficient) controls two growth rules: the spontaneous growth and the road influenced growth. It determines how many times pixels are included in the random selection in order to be urbanised. This random factor controls the creation of new single urban cells separately form the already existing urban seed. Furthermore it also effects the road influenced growth. The

higher the value, the more possibility there is to find a pixel suitable for urbanisation along the transportation network.

The **breed coefficient** has influence on two growth rules as well. By controlling the new spreading centre growth, it determines whether the previously randomly urbanised cells become new spreading centres. Besides, similarly to the diffusion coefficient, it affects the road influenced growth. It determines the number of times of possible urbanisation.

The **spread coefficient** allows already existing spreading centres (more than two urbanised cells in a 3x3 pixel area) to grow by controlling the spread growth. It does not affect non-urbanised and single cells.

The topology of an area is an important factor in urbanisation, because with the increase of the terrain's steepness, construction becomes more and more difficult. For this reason it is included as the **slope parameter** in the model and is considered by all the growth rules. The areas with higher than a certain percentage of slope (21% by default) are excluded from urbanisation. For the parts not excluded this coefficient acts as a multiplier: the higher value it has the smaller probability steeper slopes have to be urbanised. On the other hand when the value is small the percent of the slopes has less effect on the probability of urbanisation.

The **road gravity coefficient** is the fourth parameter that controls the road influenced growth. It determines the maximum search distance to find a road near a selected pixel. With the maximum value of 100 this distance is 1/16 of the image dimensions (the sum of the rows and columns). By reducing the parameter the search distance will be reduced proportionally.

4) Self-Modification

The model is allowed to alter its coefficients after each growth cycle, based on the growth rate of that year in order to show rapid and depressed growth rate trends. This is possible due to a second level of growth rules and four parameters that can be set by the user: critical high, critical law, boom and bust parameter. When the growth rate is high and the urbanised area is expanding the diffusion, breed and spread coefficients are

increased to allow more rapid growth. When the growth rate is reduced the same coefficient values are cut to show the depression.

The growth rate is calculated for each year as the percent of the newly urbanised pixels out of the total number of urbanised pixels. Examining this rate we can categorise the growth into three types: rapid, normal and little growth. The range of the growth rate for the different types is defined by the critical high and critical low values. When the rate is higher than the critical high the diffusion, spread and breed coefficients are multiplied by the boom, which is a multiplier greater than one set by the user. When the rate drops below the critical low value, by multiplying the same three coefficients by the bust (value less than 1) the growth will drop even more. Between the two critical values is the normal growth. In this case the road gravity is increased by the percent of the road network, the slope resistance is increased by 0.2 percent of the urban land available and if the average slope is greater than 10 percent the spread coefficient is increased.

5) Deltatrons

Besides urban growth modelling, the SLEUTH model is also able to predict land use change with the help of deltatrons. The driver of land use change is urbanisation. Changes in land use depend on the number of newly urbanised pixels at each growth cycle. Urbanised pixels cannot change to any other class, as well as the pixels of the excluded layer and the ones already marked with a deltatron are ignored. Deltatrons are created when a change occurs to prevent the pixel from further changes in their life cycle and to encourage similar transitions in its neighbourhood.

The probability of change between classes is calculated with the help of a two-dimensional matrix. This matrix includes the number of cells per year that were changed from one land use class to another. When a pixel is selected for change, a class with a similar average slope value with that of the selected pixel has preference.

Land use transition takes places in two phases in the model. In the first phase random cells are selected (number equals to that of the newly urbanised cells of that cycle) and are examined whether they are available for land cover change. In case an available pixel is found two land use classes are chosen randomly and their average slope is compared to the selected pixel’s slope. The class with more similar slope is chosen and the probability of change from the pixel’s class to the new class is examined

with the help of the transition matrix. The transition occurs only if the transition probability is greater than a randomly drawn number. If it is not the case, another pixel is selected for the process. After phase one, the changed pixels are marked as deltatron with a value of 1, which refers to the lifecycle age.

In phase two the neighbourhoods of recently changed pixels are encouraged to transform as well. If a pixel has at least two deltatron neighbours, transition will be attempted to the land use class of the neighbours. The probability is tested the same way as in phase one. If the random number is smaller than the transition probability, transition will be implemented. At the end of the phase, all new transitions are added to the deltaspace as deltatrons with the age of one and the previous deltatrons' age increases by 1. Deltatrons decay after a set number of years and they became available for transition again. (Candau and Clarke, 2000)

3.5.4 Creation of the scenarios

After the calibration of the SLEUTH model, the growth coefficients were analysed to find a way of creating the four types of scenarios. The increase in the diffusion coefficient results in more isolated scenarios due to the increase in single urbanised cells, while the spread coefficient controls the compactness of the scenarios. It can only initiate growth around already existing urban centres. The breed coefficient controls the urban growth around the new spreading centres. Without the breed coefficient the new urbanised cells cannot start growing. By choosing a set breed variable for all the scenarios and changing the diffusion and spread variables in a predefined order, a series of scenarios were created demonstrating isolated and compact characteristics depending on the greatness of the two variables. The combination of the two growth types is the combined growth, which demonstrates characteristics of both two types with equal diffusion and spread values. The breed variable was set to 75 so that some new urban cells can become spreading centres and not only single cells appear in case of the isolated scenarios. The other two variables were changed between the minimum and maximum values with a step of 25 in all 25 possible combinations. In addition to this, eight more scenarios were created in a way that the sum of the two variables is always 100. Figure 3.5 shows all 33 scenarios in a Diffusion-Spread coordinate system.

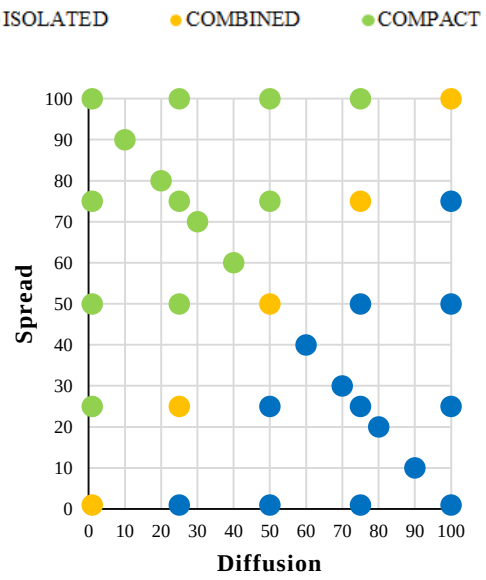

Figure 3.5 Scenarios in a diffusion-spread coordinate system

The road based scenarios were the most difficult to simulate, as they are effected by four of the coefficients. Table 3.4 demonstrates the effects induced by the diffusion, breed and spread coefficients on the road influenced growth. It was measured by comparing the road influences urban growth in the scenarios with the variables set to 1, 50 and 100. The smaller the diffusion and spread variables are, the higher the urban growth is. The decrease in the spread coefficient simulates great increase in road influenced urban growth: by changing from 100 to 50 the spread variable, the road growth doubles, and the road growth simulated by spread of 1 is more than 10 times greater than by spread of 50. To ensure high road influenced urban growth, the spread coefficient was kept 1 in all road based scenarios. The breed variable simulates more road influenced growth when greater. However, since the difference between using the maximum and 75 is not significant, the five road based scenarios were conducted with constant breed of 75 following the settings of the previous scenarios. Keeping the breed, spread and road coefficients constant the only changing variable was the diffusion, varying between 1 and 100 by steps of 25. These five scenarios only differ from the isolated-compact scenarios in the road coefficient, which is increased to the maximum from 1 to emphasise road gravity. Due to this similarity it cannot be marked separately on the diffusion-spread graph. It does not show differences in these two coefficients.

Urban area of 98000 pixels, breed 75, road 100									
diff	**100**			**50**			**1**		
spread	**years**	**road growth**	**% of all growth**	**years**	**road growth**	**% of all growth**	**years**	**road growth**	**% of all growth**
100	6	248,6	0,64	7	257,45	0,62	7	205,93	0,53
50	10	421,09	1,08	11	445,23	1,14	13	448,65	1,12
1	53	4807,99	18,14	82	6566,56	23,24	270	10703,13	29,56

Urban area of 98000 pixels, spread 1, road 100									
diff	**100**			**50**			**1**		
breed	**years**	**road growth**	**% of all growth**	**years**	**road growth**	**% of all growth**	**years**	**road growth**	**% of all growth**
100	43	5188,41	20,57	69	7230,81	26,21	241	12035,92	33,81
75	53	4807,99	18,14	82	6566,56	23,24	270	10703,13	29,56
50	66	4090,86	15,05	103	5670,26	19,14	314	8929,34	24,01
1	142	378,47	1,22	225	551,87	1,62	does not reach area till 2500		

Table 3.4 The influence of the diffusion, breed and spread coefficients on the road influenced urban growth (road influenced urban growth in pixels, and the percent of this growth compared to all the urbanised pixels)

The influence of the topology was omitted by setting the slope coefficient to a constant 1, since the average slope is less than 3%. The slopes were only considered by the exclusion of areas with steeper than 21 slope percent. The only hilly area reaching this criterion is in the North-West corner of the study area as it is visible in the slope and hill shade inputs (Figure 3.3 e, f).

The self-modifying capability of the model was also deactivated to avoid changes in the manually set coefficients. The self-modifying parameters let the model adjust the coefficients based on the amount of growth measured after each life cycle. Without the exclusion the road and slope coefficients demonstrated especially great changes, which caused difficulties in creating road based scenarios. Setting all six parameters (critical low and high, boom and bust, road and slope sensitivity) to 0 prevented the set coefficients from changing at the end of each growth cycle depending on the amount of growth. They remained constant throughout the whole process.

The spread coefficient initiates a more rapid growth than the diffusion. This results in differences in the amount of urban growth between compact and isolated scenarios within a set number of years.

Since the aim was to compare the fragmentation of the scenarios, it was important to omit these differences. This was possible by calculating the amount of urban growth that should occur in 50 years and simulate each scenario so that this level of urbanisation is reached, instead of computing each scenario in 50 years. The latter method would have resulted in differences in the amount of urbanised area, while the former gives similar urban growth suitable for more accurate comparison. The calculations were based on the urban class of the land use cover, assuming that the average growth per year would remain similar in 50 years as it was between 2006 and 2012. Terando et al. (2014) explains this as the business as usual growth (BAU), indicating that the growth in the future is considered equal to the growth rate observed in the past. The difference between the two UA dates (2006 and 2012) in urban growth is 2.315 km^2 (2573 pixel) which means a 0,386 km^2 (428.83 pixel) growth per year. The urban area covers 68.845 km^2 (76494 pixels) in 2012 so assuming the same average growth, 50 years later in 2062 the urbanised area will be approximately 88.142 km^2 (97935.67 pixels).

The prediction mode of the SLEUTH model works similarly as the calibration. However, here not a range of values are assigned to each coefficient, but one selected number. The prediction was conducted for all 38 scenarios with a number of iterations so that for each scenario the iteration with the most similar area could be selected. The model generates image and statistical output in prediction mode. The statistical data includes the total number of urbanised pixels in each year. With the help of this information the simulated land use cover output with the proper amount of urbanised area was selected for each scenario. These 38 images were used in the analysis. There is an example scenario at the end of this chapter (Figure 3.6) and one scenario of each growth type can be found in APPENDIX 2.

The output scenarios were named according to the coefficients applied in prediction. Since the slope is always 1, the breed is 75 and the road is also 1 in all but 5 scenarios, to keep the names simple, only the diffusion and spread coefficients were used in the label. To differentiate the road based scenarios they were given a sign (*). For example the name of the compact scenario with max spread and minimum diffusion is 1-100 (diff:1, breed:75, spread: 100, slope:1, road:1) and an example road based scenario looks like: 100-1* (diff: 100, breed: 75, spread: 1, slope:1, road: 100).

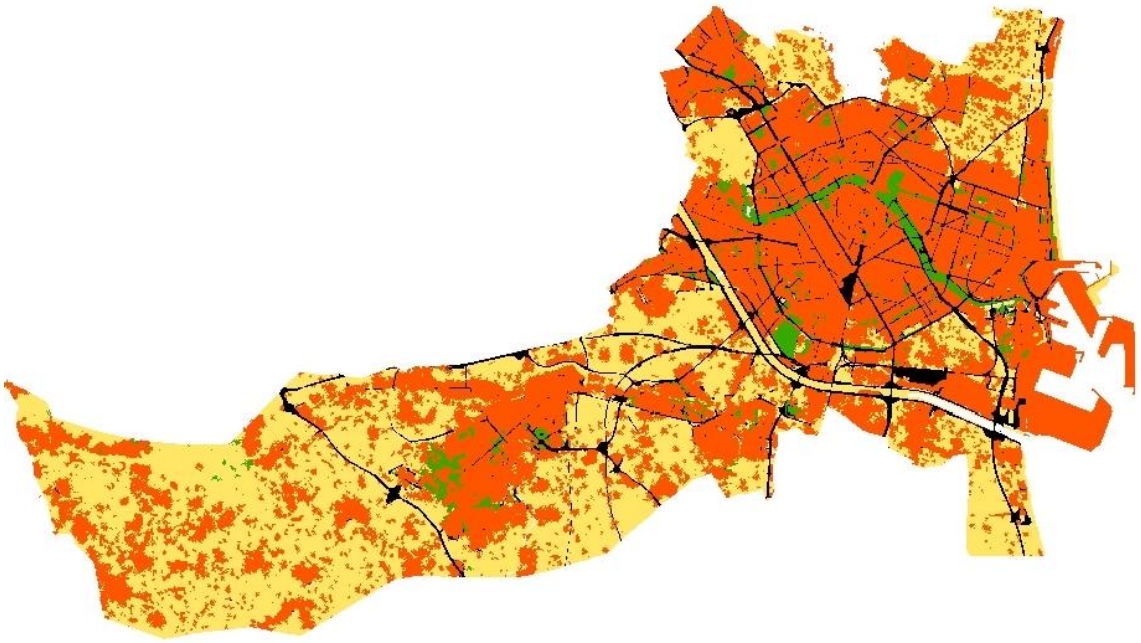

Figure 3.6 Output scenario of the SLEUTH model: combined growth type (70-30)

3.6 Application of fragmentation indices

IndiFrag is a processing tool written in the programming language Python for ArcGIS. It was developed to characterize landscape fragmentation based on LULC data (Sapena and Ruiz, 2015a). The tool works with georeferenced vector data as a result both the reference and simulated maps had to be adapted to these conditions. Figure 3.5 illustrates the steps of the preparation of the SLEUTH output data for IndiFrag and of the calculation of the metrics. In the first step the simulated maps in raster format were georeferenced with the help of the reference maps of 2012. As they were originally created from georeferenced vector data, they have a coordinate system. Their projection files were simply added to the SLEUTH model scenarios. Next, both the reference and simulated maps were converted to vector format to meet the requirements of the IndiFrag tool. The tool can be accessed from ArcMap and requires only a shapefile of the objects in polygon format with their classification in order to operate. The only metric that requires an additional point feature is the Radius Dimension (DimR). It measures the centrality of land use patterns with the help of a central point. In this case it is an approximated centroid of the urban class extracted from Corine Land Cover 2000 (Eurostat, 2017).

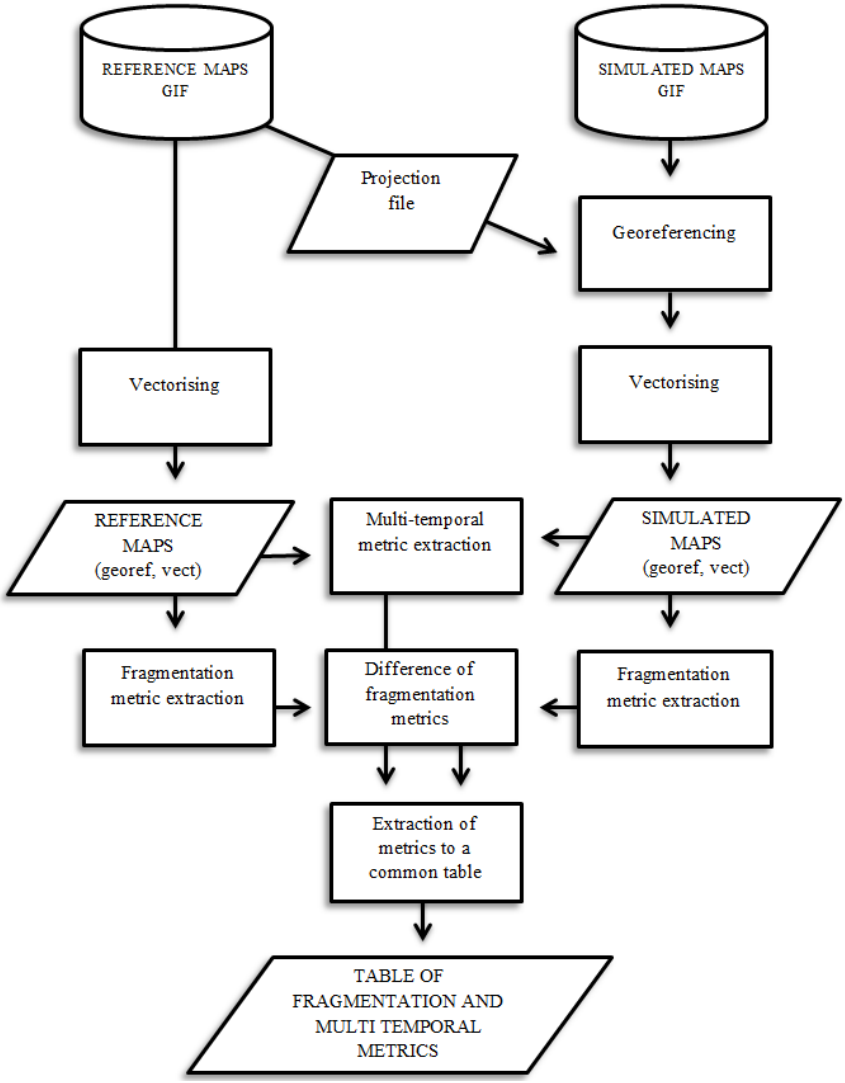

Figure 3.7 Work flow of the application of fragmentation and multi-temporal indices to SLEUTH output data

The indices can function at three different hierarchical levels from lowest to highest: object, class and super-object (Sapena and Ruiz, 2015a). The lowest level was not considered, since at this level only the size and shape of the spots are characterized by the metrics, which was not interesting to be analysed in this study. The class level describes the characteristics of the objects within the same class, in this case the urban class (U). The highest level is the super-object (SO) level, where the relation between classes is observed within the boundaries of super-objects. In this study the super-object covers the whole study area, because urban growth was not examined at district level.

The 31 fragmentation indices (FI), from which 24 can be applied to super-object level and 23 to class level, describe a variety of properties: area, perimeter, shape, aggregation, diversity and contrast. These metrics examine the state of fragmentation at a certain point in time. In order to be able to measure changes, the indices have to be first calculated separately for the simulated and historical scenarios and then compute the difference between them. In addition there exist also multi-temporal fragmentation indices (MI), which directly analyse changes of the land use pattern (Sapena and Ruiz, 2015b). This multi-temporal module of IndiFrag contains 15 metrics. As the last step these were conducted for each scenario. Appendix 3contains the list of metrics with their names used in the study.

In the end the calculated metrics for each scenario were extracted from the attribute table of each shapefile into one common table (Appendix 4). This includes the fragmentation change of the whole study area (24) and of urban class (23) and multi-temporal metrics for urban class (12).

3.7 Selection of indices

From the 59 metrics applied to the scenarios many shows similarities, as they describe similar properties. To prevent redundancy the metrics not providing new information on the characteristics were eliminated. All the scenarios were created in a way that the areas are close to equal in order to be able to compare the growth types accurately. As a result the metrics informing about the area did not show significant change between the scenarios. If they did, it is due to the small differences in the areas that could not be avoided. These were eliminated from further analyses, for example: Area, Perim, DU, Area_U, DC_U, DD_U, CP, RC, Ac, At and Ar all depend on urban area. Other metrics eliminated are RAMPA, IF, DF due to the lack of information they provide at SO level. They characterize the shape of objects of every class. Some metrics were eliminated, because there are other metrics providing very similar information. For example CU is the same as CC; USHAN and SIMP resemble to DSHAN; GC_U, IS_U and COHE to TEM and IF_U, DF_U to RMPA and DFP. Finally only 33 metrics remained all together: 13 fragmentation metrics of the super objects, 15 of urban class and 5 multi-temporal.

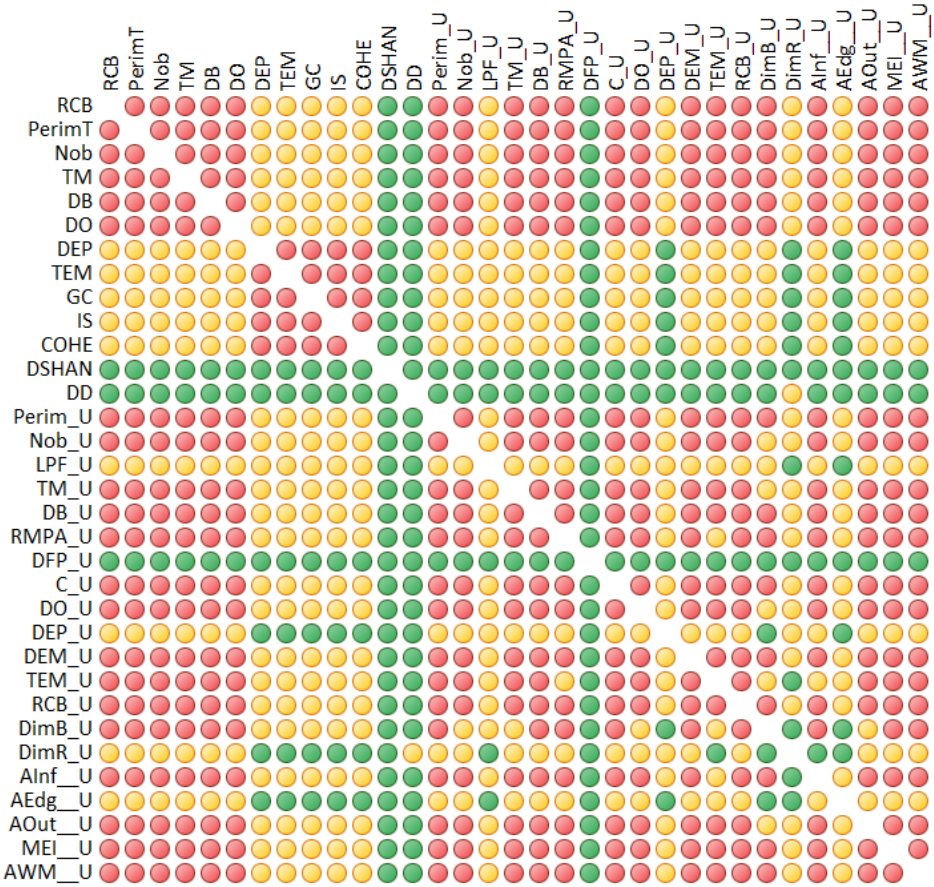

Figure 3.8 Correlation coefficients of the fragmentation metrics. Red: very high (|ρ|>0.9), yellow: high (0.7<|ρ|<0.9), green: medium and low (|ρ|<0.7)

As a second step the high number of indices and redundant information still present in the database were reduced by applying correlation analysis to the complete set of 33 elements (Figure 3.8). *"Correlation measures the direction and strength of the linear relationship between two quantitative variables."* (Moore et al., 2014) The correlation can range between -1 and 1. The negative values show negative correlation and the positive values positive correlation. Correlation close to 0 indicates a weak relation between the variables. The closer the correlation is to 1 or -1, the stronger the relationship is. There are 7 metrics that did not show high correlation with any other metric: DSHAN, DD, LPF_U, DFP_U, DO_U, DEP_U and DimR_U. These were kept. The highly correlating metrics, with a correlation coefficient greater than 0.9, were examined. From each group of correlating metrics one was kept for further analysis and the rest were omitted to prevent the influence of redundant data. For example DEP, TEM, GC, IS and COHE show high correlation between themselves but not with other

metrics. Except for TEM, all the other metrics from the group were eliminated. The remaining metrics are: TEM, DSHAN, DD, LPF_U, DFP_U, DO_U, DEP_U, DimB_U, DimR_U and AEdg_U.

3.8 Classification and validation

The methodology of the classification of the scenarios into the growth types based on the previously calculated fragmentation indices is explained here together with the method of validation of these classifications. First the discriminant analysis is introduced, which is followed by the cluster analysis. Their results are evaluated by cross validation and regression analysis, respectively.

3.8.1 Discriminant analysis with cross validation

The previously selected 10 metrics were used in the classification procedure. Discriminant analysis is a commonly used supervised classification method, thus requires a set of seed observations with known characteristics. It distinguishes between the classes using discriminant functions, which are linear equations of the variables. The functions calculate the probabilities of belonging to each growth type for each scenario. The 38 scenarios were classified to the growth type with the highest probability. In case of stepwise selection only the most important metrics are selected for the classification with the help of the F-to-enter variable. It starts the model with only one variable and at each step the statistically most significant variable is added. The statistical significance is defined by the F-value. When for a certain metric it is greater than the F-to-enter variable, it will be added to the model. The metrics later can be removed if their F value falls below the F-to-remove criterion. Discriminant analysis was applied to all three cases, which means that in each case the growth types set as classification factor were changed according to the cases (Case 1: isolated, compact, Case 2: isolated, compact, combined, Case 3: isolated, combined, road based). To see how each additional metric influence the accuracy of the classification, the stepwise forward analysis was applied with 0 F-to-enter level, so that one by one all the metrics will be included in the end. Although the maximum overall accuracy can be reached with more metrics, considering the small sample size of the database only fewer variables were selected for further analysis. This way over-fitting is avoided and redundancy in the variables is reduced.

The variables with a greater F value than 4 were selected, which means the first three steps of the forward selection. The rest of the variables demonstrate very low significance in classification thus they were omitted.

The results were validated using cross-validation technique because of the reduced number of scenarios. This method does not require the separation of the already small data set into separate training and test sets, instead divides the data into subsets and conducts the analysis on one set (as training set) and validates this on another subset (as testing set). This can be performed multiple times by changing the testing and training sets and at the end the average of the accuracy for the rounds is calculated. The 38 scenarios were randomly divided into four sets (two of 10 and two of 9 scenarios). During the validation always three different sets were used in the discriminant analysis as training set and the fourth as testing. The average accuracy of the 4 analysis on the testing set estimates the goodness of fit of the metrics.

3.8.2 Cluster analysis and coefficient of determination

The scenarios were also classified into two groups using unsupervised classification. Because of the small size of the database, to avoid overfitting, only the most significant metrics were used to conduct this analysis. The three metrics selected by the stepwise forward selection of the discriminant analysis were used (Case 1). In cluster analysis there are no samples given for each class to help the algorithm distinguish between groups of observations. *"Cluster analysis groups data objects based only on information found in the data that describes the objects and their relationship. The goal is that the objects within a group be similar (or related) to one another and different from (or unrelated to) the objects in other groups"* (Tan et al., 2015). The objects are clustered by calculating distances between them based on the variables. There is a great diversity of cluster analysing algorithms available and depending on the dataset different methods can work more successfully (Estivill-Castro, 2002). From the 7 methods that STATGRAPHICS offers k-means proved to be the most efficient algorithm. In this algorithm a scenario is selected for each cluster as a seed and the rest of the scenarios are matched to the closest cluster using the Squared Euclidian distance:

$$d(x, y) = \sum_{i=1}^{p}(x_i - y_i)^2, \quad (1)$$

where p is the number of metrics (p=3).

When all the objects are assigned to a cluster, the centroids are calculated and each scenario is examined one by one to see whether it is closer to a centroid of another cluster than its own. If so, it is assigned to the other cluster and the centroids are recalculated before starting the supervision of the other scenarios.

After determining a cluster for each scenario, their distance was calculated from the two centroids to evaluate the accuracy of the analysis. This value was compared to the compactness of the scenarios. The degree of compactness (DoC) was calculated based on the diffusion (D) and spread (S) coefficients of the SLEUTH model. Figure 3.9 explains the conversion of the scenarios from the diffusion-spread coordinate system to the degree of compactness. The distance of the scenarios to the red line can be calculated for each point as the height of an isosceles right triangle ((S-D)/√2). The scenario with the lowest degree of compactness is 100-1, thus the red line of 0 compactness was shifted here. This means that to all the calculated distances to the red line 70,0036 has to be added (distance between 0 compactness and red line) in order to get the degree of compactness ranging between 0 and 140 and not -70 and 70. The following equation shows the calculations:

$$\mathrm{DoC} = \frac{\mathrm{S} - \mathrm{D}}{\sqrt{2}} + |(S_{lowest} - D_{highest})/\sqrt{2}| \quad (2)$$

where

$$|(S_{lowest} - D_{highest})/\sqrt{2}| = |(1 - 100)/\sqrt{2}| = 70.0036 \quad (3)$$

The maximum spread with minimum diffusion value is the highest level of compactness (140) and spread of 1 and diffusion of 100 is the lowest (0). All the other scenarios are assigned a value between them. The combined scenarios are in the middle with compactness of 70. The compactness of the road based scenarios equals to that of the scenarios with equivalent diffusion and spread values.

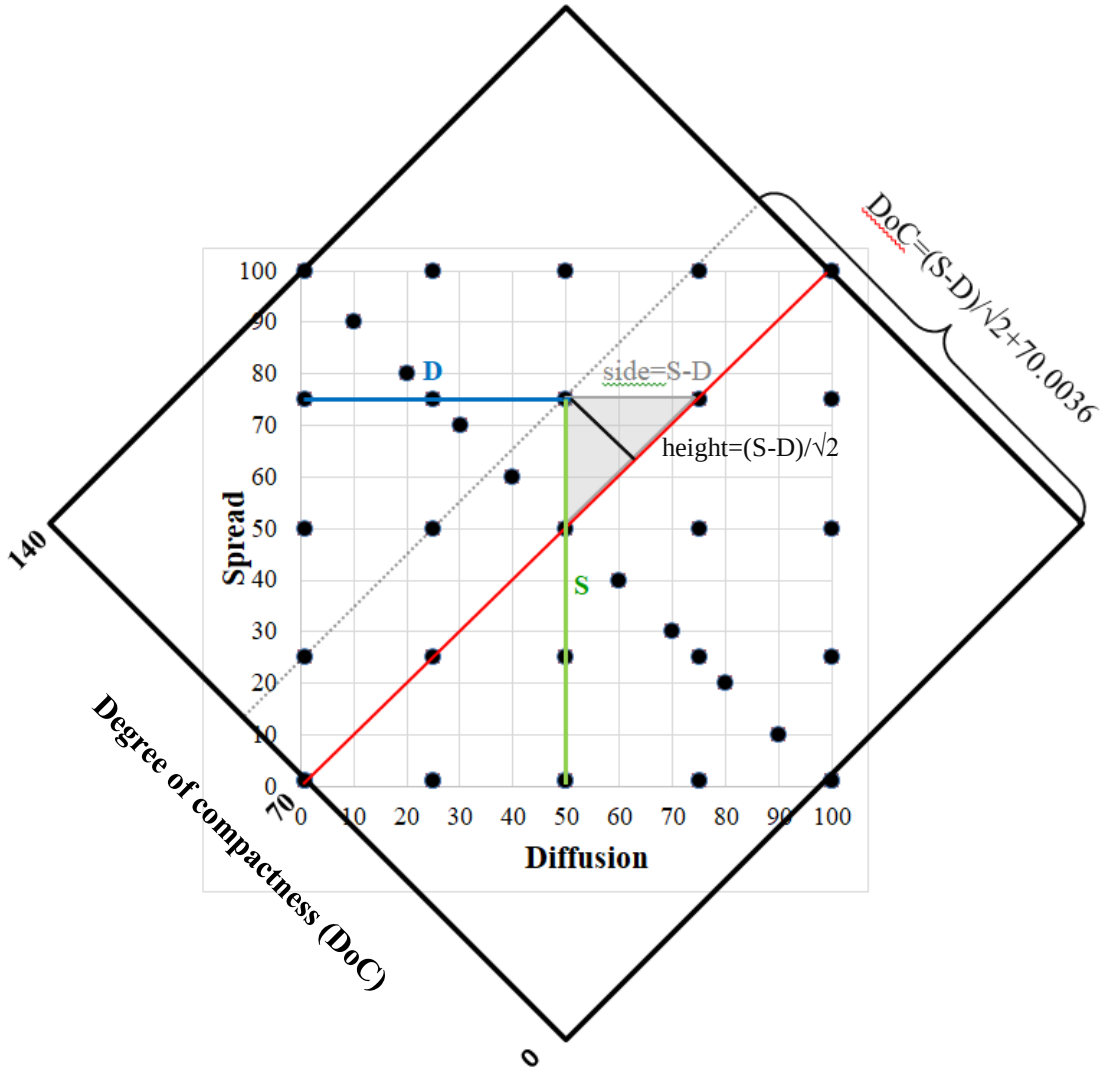

Figure 3.9 Conversion from diffusion-spread coordinate system to the degree of compactness

Finally, as an evaluation of the cluster analysis, the relation between the compactness and the distances to the two centroids were explored by regression analysis. "*Regression analysis is a statistical technique for modelling and investigating the relationship between two or more variables"* (Montgomery and Runger, 1999). The simple linear regression analysis is suitable for two variables showing linear relationship in a way that the dependent variables are normally distributed over the independent variables. In the single regression analysis computed on the two variables the cause is the distance to the centroid serving as the independent variable and the effect (dependent variable) is the degree of compactness. The regression coefficients were estimated by the method of least squares. *"The least-squares regression line of y*

on x is the line that makes the sum of the squares of the vertical distances of the data points from the line as small as possible. (…) It looks at the distances of the data points from the line only in the y direction. So the two variables x and y play different roles in regression" (Moore at al., 2014). The goodness of fit was computed by the coefficient of determination, an output of the regression analysis used commonly to examine the accuracy of a regression model. *"It is the square of the correlation, the fraction of the variation in the values of y that is explained by the least-squares regression of y on x"* The squared correlation gives 1 when all the variation in one variable can be described by the linear relationship with the other variable. The decrease in the coefficient of determination shows the decrease in the accuracy of the regression line describing the relation between the two variables.

4 RESULTS AND DISCUSSION

The aim of this chapter is to demonstrate and explain the results of the classification of the scenarios into the growth types, including the results of the validation as well. These were calculated following the methodology described at the end of the previous chapter.

4.1 Results of the classifications

The results of the stepwise forward discrimination analysis applied to the three cases are shown in Figure 4.1 and Table 4.1. Figure 4.1 presents how the overall and class accuracies of the supervised classification are changing while introducing new variables. Table 4.1 contains the outcome of the analyses on the three cases (MP) after adding all ten metrics compared to the real classification (R). The scenarios are classified into the growth type to which the model assigns the highest probability (%).

In Case 1 the two groups are discriminated with an overall accuracy of 93.75% already after introducing the first variable and to improve that five more variables have to be added, reaching the maximum accuracy of 1 with seven metrics. The accuracy of the combined scenarios in Case 2, the transition between the isolated and compact classes, hardly surpasses 50%. The combined scenarios with lower coefficients (1-1, 25-25 and 50-50) are correctly classified, but with high spread and diffusion variables the scenarios are assigned to the compact class (75-75, 100-100). The spread coefficient, which defines the compactness of the scenarios, shows greater growth per year than the diffusion coefficients. As a result the high spread values let the scenarios reach the required area before the diffusion coefficients could create isolated urbanised areas and represent evenly the isolated characteristics of the combined scenarios. Since the discrimination of the other two scenarios remains highly accurate, the overall accuracy stays as high as 70-90%. In Case 3, the 5 road based scenarios (1-1*, 25-1*, 50-1*, 75-1*, 100-1*) cannot be distinguished from the isolated and compact scenarios with the

same spread and diffusion values (1-1, 25-1, 50-1, 75-1, 100-1). Although Figure 4.1 demonstrates high accuracy for the road based scenarios (80-100%), Table 4.1 proves that it is at the cost of the accuracy of the other growth types. The classification of 4 of the 5 road based scenarios correspond to the 4 scenarios with the same spread and diffusion values, but 0 road coefficient: 25-1, 25-1* classified as isolated and 50-1, 50-1*, 75-1, 75-1*, 100-1 and 100-1* are classified as road based. A reason for this might be that the SLEUTH model does not allow changing the influence of the road enough to make a notable difference. Another explanation might be that the road influenced growth has too similar growth pattern to the isolated growth, similarly expanding from several spreading centres. As a result in fragmentation the difference is too small to be recognised by the metrics.

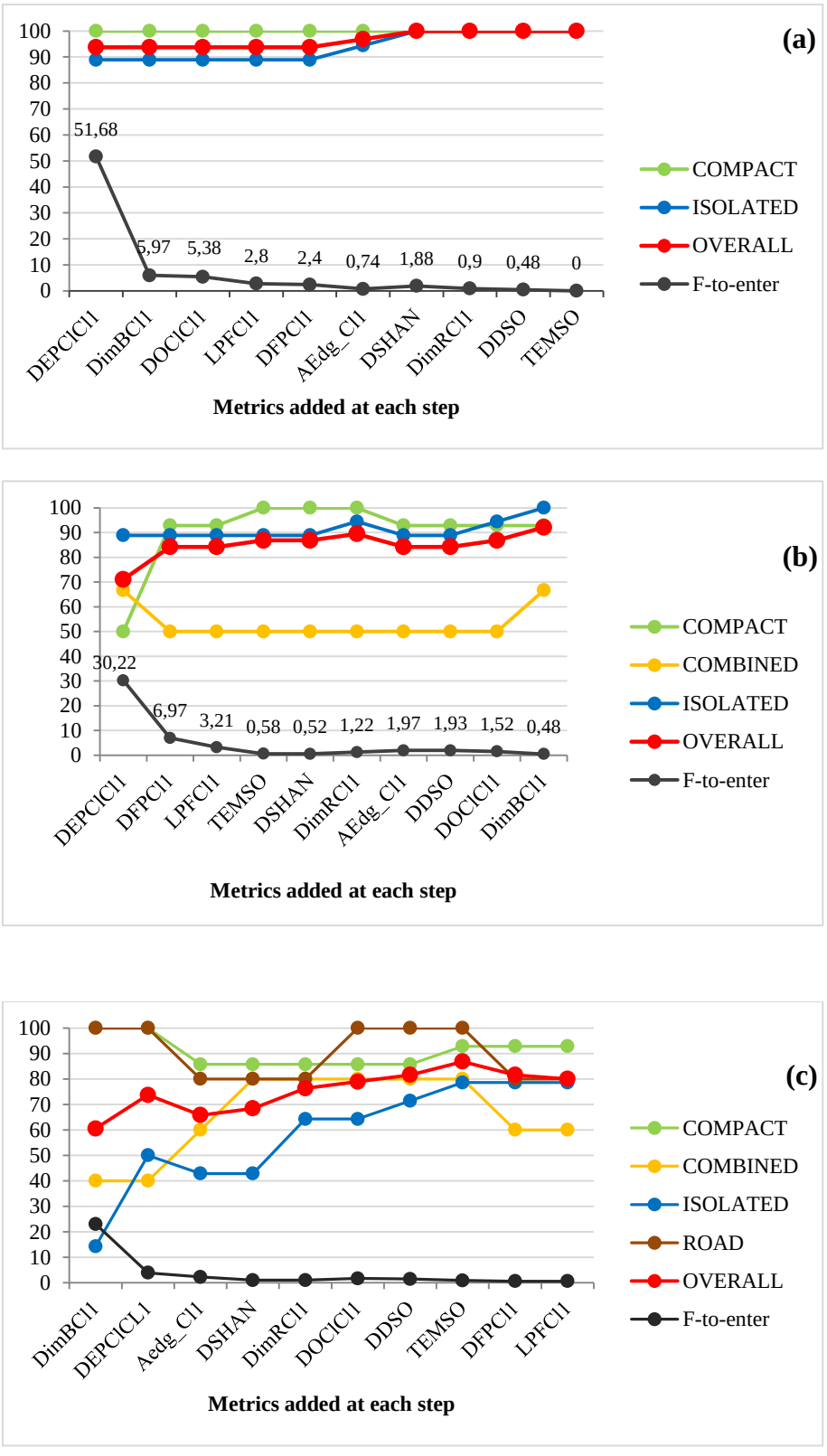

Figure 4.1 The accuracy and F-to-enter value of the Stepwise Discriminant Analysis with Forward Selection at each step adding one more metric **(a)** Case 1 **(b)** Case 2 **(c)** Case 3

SLEUTH	Case 1			Case 2			Case 3		
	R	MP	%	R	MP	%	R	MP	%
100_1	I	I	1	I	I	1	I	*R	0.768
75_1	I	I	1	I	I	0.99	I	*R	0.974
50_1	I	I	1	I	I	1	I	*R	0.564
25_1	I	I	1	I	I	0.999	I	I	0.591
1_1		I	1	X	X	1	X	X	0.999
90_10	I	I	1	I	I	1	I	I	0.852
80_20	I	I	0.997	I	I	0.98	I	I	0.895
100_25	I	I	1	I	I	0.994	I	I	0.977
75_25	I	I	1	I	I	1	I	I	0.99
50_25	I	I	0.997	I	I	0.725	I	I	0.805
25_25		C	0.914	X	X	0.894	X	X	0.892
1_25	C	C	0.983	C	C	0.928	C	C	0.889
70_30	I	I	0.996	I	I	0.973	I	I	0.914
60_40	I	I	1	I	I	0.986	I	I	0.956
100_50	I	I	0.982	I	I	0.994	I	I	0.923
75_50	I	I	0.791	I	I	0.789	I	I	0.801
50_50		I	0.656	X	X	0.49	X	*I	0.497
25_50	C	C	0.706	C	*X	0.79	C	*X	0.807
1_50	C	C	1	C	C	0.917	C	C	0.815
40_60	C	C	0.985	C	C	0.788	C	C	0.673
30_70	C	C	0.997	C	C	0.794	C	C	0.687
100_75	I	I	0.835	I	I	0.446	I	I	0.543
75_75		C	1	X	*C	0.85	X	*C	0.646
50_75	C	C	0.999	C	C	0.671	C	C	0.611
25_75	C	C	0.999	C	C	0.944	C	C	0.937
1_75	C	C	1	C	C	0.993	C	C	0.991
20_80	C	C	1	C	C	0.993	C	C	0.99
10_90	C	C	1	C	C	0.995	C	C	0.992
100_100		C	0.997	X	*C	0.609	X	X	0.54
75_100	C	C	1	C	C	0.942	C	C	0.817
50_100	C	C	1	C	C	0.853	C	C	0.778
25_100	C	C	1	C	C	0.949	C	C	0.933
1_100	C	C	1	C	C	0.938	C	C	0.911
100_1*	I	I	1	I	I	1	R	R	0.996
75_1*	I	I	1	I	I	1	R	R	0.658
50_1*	I	I	1	I	I	1	R	R	0.888
25_1*	I	I	1	I	I	0.95	R	*I	0.532
1_1*		I	0.996	X	X	0.999	R	R	0.996
Global Ac.	100			92.11			81.58		

R
Real classification

MP
Most probable class

%
Probability of MP

I
isolated

C
compact

X
combined

R
road

Global Ac.
Global Accuracy

Table 4.1 Outcomes of the discriminant analysis using 10 metrics (Case 1-3)

It is visible that the more growth types there are included in the classification, the lower the accuracy of the overall classification is. In other words, it is more difficult to assign the scenarios according to the real classification of more growth types. The fragmentation metrics distinguish between the two classes of growth of the first case the most accurately. In the following analyses the accuracy of the classification into these two classes is examined. Based on the stepwise forward selection on Case 1 (Figure 4.1), the three metrics with the highest F value (greater than 4) were DEP_U, DimB_U and DO_U, which were kept for further classification and analysis, since they demonstrate high significance in classification. The results of the discriminant analysis applied on Case 1 using three metrics can be seen in Figure 4.2.

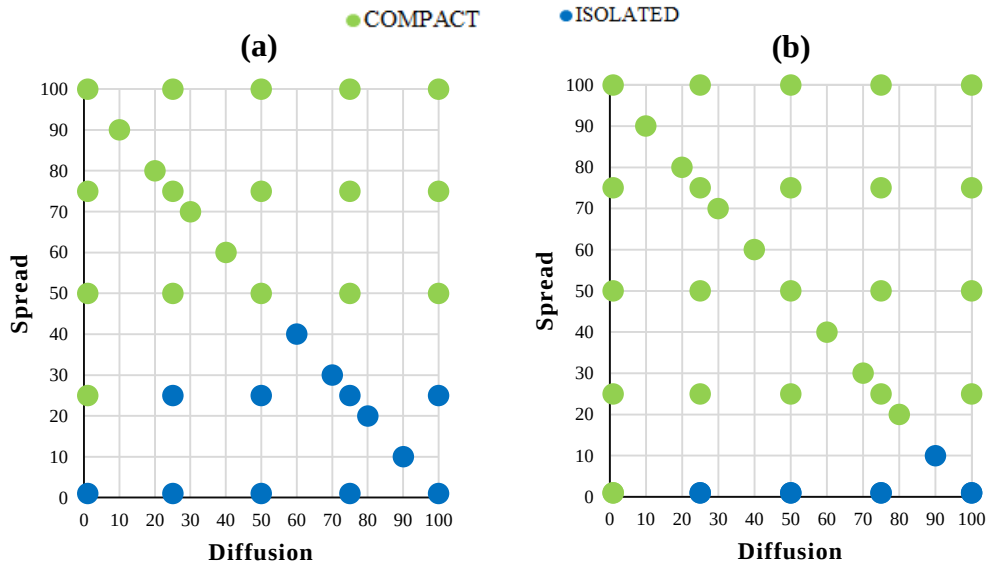

Figure 4.2 Results of the classification in a diffusion-spread coordinate system identifying two growth types using three metrics **(a)** Discriminant analysis **(b)** Cluster analysis

Comparing the results of the classification by discriminant and cluster analysis discriminating two classes (Case 1) in Figure 4.2, it is visible that cluster analysis without the seed scenarios' help recognises less isolated scenarios than the discriminant analysis: only the scenarios with less than 20 spread coefficient.

Table 4.2 contains the results of the cluster analysis: the classification and the centroids of the clusters. Figure 4.3 demonstrates the spread of the scenarios in the three

dimensional coordinate system of the three metrics and locates the two centroids based on which the classification depends. Half of the isolated scenarios are very near the centroid of this cluster while four are located further (group 1 and 5), but still visibly closer to this centroid than to the compact centroid. The compact cluster contains the majority of the scenarios, most of them closely surrounding the centroid, while one group is further spread opposite direction of the isolated cluster (group 2) and two groups of compact scenarios are between the two clusters (group 3 and 4). Group 2 is the furthest from the isolated centroid containing scenarios with high spread and low diffusion coefficients: 25-75, 20-80, 1-75 and 1-100. Group 4 includes the two scenarios with minimum spread and diffusion coefficients, located between the two centroids, but closer to the compact cluster. Group 3 includes the originally isolated scenarios that were assigned to the compact cluster, located very close to the isolated centroid, almost halfway between the two centres. The graph demonstrates the strong similarity between the road based scenarios and their non-road-based equivalent always closely located: 1-1 and 1-1*, 25-1 and 25-1*, 50-1 and 50-1*, 75-1 and 75-1*, 100-1 and 100-1*. This similarity in the metrics prevents them from being classified separately. The rest of the combined scenarios not included in group 4 (25-25, 50-50, 75-75, 100-100) are located right next to the compact centroid surrounding it by every side, some closer, some further from the isolated cluster making it difficult to be separately clustered form the rest of the compact scenarios surrounding them.

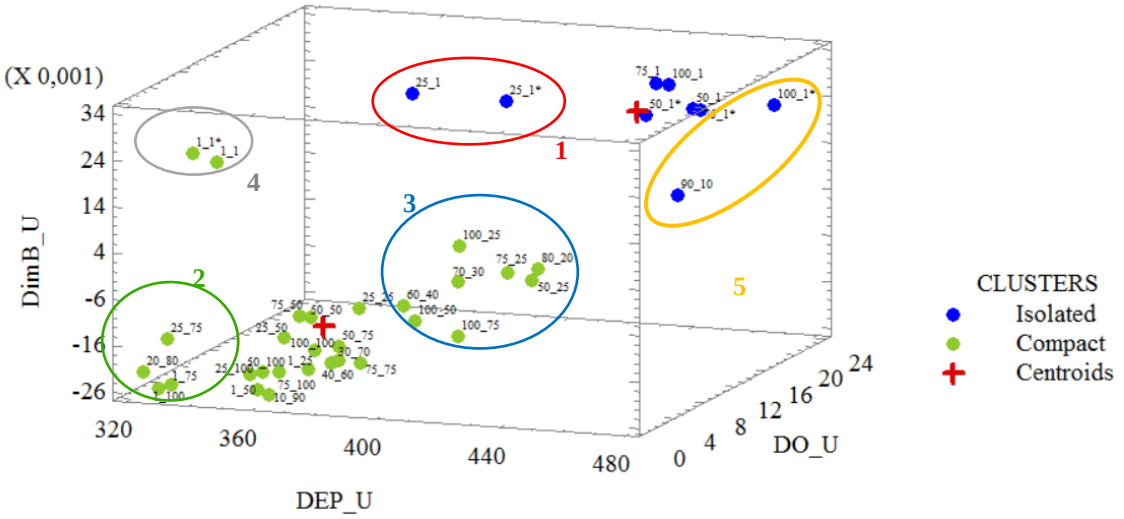

Figure 4.3 Results of cluster analysis in STATGRAPHICS

SLEUTH	DEP_U	DimB_U	DO_U	CLUSTER
100_1	440,73	0,02747	21,212	1
75_1	439,39	0,02858	20,1433	1
50_1	455,85	0,02554	18,1924	1
25_1	374,09	0,02809	14,7354	1
90_10	466,62	0,01289	11,7423	1
100_1*	476,43	0,0254	20,5588	1
75_1*	454,39	0,02369	19,9233	1
50_1*	442,19	0,0242	17,6354	1
25_1*	404,34	0,02769	14,7407	1
1_1	338,75	0,02123	3,39864	2
80_20	430,88	-0,00133	8,014	2
100_25	407,61	0,00302	7,2401	2
75_25	425,88	-0,00088	6,0791	2
50_25	436,37	-0,00104	4,8301	2
25_25	385,65	-0,00759	2,86616	2
1_25	374,17	-0,01972	0,91947	2
70_30	410,46	-0,00329	5,8529	2
60_40	396,57	-0,00795	4,3214	2
100_50	397,53	-0,01218	5,4478	2
75_50	363,75	-0,01129	4,01614	2
50_50	369,69	-0,01051	3,109	2
25_50	363,93	-0,01421	1,9364	2
1_50	358,79	-0,02446	0,61354	2
40_60	377,8	-0,01945	2,54278	2
30_70	381,51	-0,01822	1,90145	2
100_75	414,68	-0,01333	4,1429	2
75_75	384,28	-0,02029	3,66398	2
50_75	379,61	-0,01598	2,79085	2
25_75	326,57	-0,01613	1,84951	2
1_75	330,9	-0,02462	0,58483	2
20_80	320,25	-0,02307	1,27178	2
10_90	361,63	-0,02574	0,95966	2
100_100	371,05	-0,01771	3,13727	2
75_100	359,83	-0,02281	2,9699	2
50_100	357,32	-0,02174	1,87225	2
25_100	354,5	-0,02201	1,27767	2
1_100	327,39	-0,02566	0,45154	2
1_1*	330,3	0,02257	3,67573	2

CENTROID			
CLUSTER	DEP_U	DimB_U	DO_U
1	439,337	0,024839	17,6537
2	373,712	-0,01222	3,16334

Table 4.2 Outcome of the cluster analysis using three metrics

4.2 Accuracy of the classifications

The result of the cross validation on the classification of the discriminant analysis, in each of the four combinations of three training sets was the same: accuracy of 94.7%. The scenarios not assigned according to the predefined growth type were 100-50 and 75-50 and the “combined scenarios” as a consequence of being ignored in Case 1. It seems that in scenarios with medium spread coefficient and high diffusion even if the later one is higher the metrics recognise the characteristics rather of a compact scenario than an isolated. Table 4.3 summarises the groups of 9-10 scenarios, their real classification and in which growth type they were classified by discriminant analysis. In each set up of three groups of training and 1 group of testing the outcome was the same.

Group	SLEUTH	GT	DEP_U	DimB_U	DO_U	CL	ACC
1	50_1	I	455,8500061	0,02554	18,19239998	I	true
	1_1		338,75	0,021229999	3,398639917	I	*false*
	80_20	I	430,8800049	-0,00133002	8,013999939	I	true
	50_25	I	436,3699951	-0,0010401	4,83010006	I	true
	70_30	I	410,459992	-0,0032901	5,8529	I	true
	75_50	I	363,75	-0,0112901	4,016139984	C	**false**
	20_80	C	320,25	-0,023070101	1,271780014	C	true
	50_100	C	357,3200073	-0,021740099	1,872249961	C	true
	1_100	C	327,3900146	-0,025660001	0,451539993	C	true
	25_1*	I	404,3399963	0,0276899	14,74069977	I	true
2	90_10	I	466,6199951	0,01289	11,74230003	I	true
	100_25	I	407,6099854	0,00301993	7,240099907	I	true
	25_25		385,6499939	-0,00759006	2,866159916	I	*false*
	1_25	C	374,1700134	-0,0197201	0,919470012	C	true
	60_40	I	396,570007	-0,0079501	4,3214002	I	true
	100_50	I	397,5299988	-0,0121801	5,447800159	C	**false**
	50_50		369,6900024	-0,0105101	3,108999968	C	*false*
	1_75	C	330,8999939	-0,024620101	0,584829986	C	true
	10_90	C	361,6300049	-0,025739999	0,959659994	C	true
	100_1*	I	476,4299927	0,025399899	20,55879974	I	true
3	75_25	I	425,8800049	-0,000880003	6,079100132	I	true
	25_50	C	363,9299927	-0,0142101	1,936400056	C	true
	1_50	C	358,7900085	-0,0244601	0,613539994	C	true
	40_60	C	377,7999878	-0,0194501	2,542779922	C	true
	100_75	I	414,6799927	-0,0133301	4,14289999	I	true
	50_75	C	379,6099854	-0,01598	2,790849924	C	true
	25_75	C	326,5700073	-0,016130099	1,849509954	C	true
	100_100		371,0499878	-0,017710101	3,137269974	C	*false*
	1_1*		330,2999878	0,0225699	3,67572999	I	*false*
4	100_1	I	440,730011	0,02747	21,21199989	I	true
	75_1	I	439,3900146	0,028580001	20,1432991	I	true
	25_1	I	374,0899963	0,02809	14,7354002	I	true
	30_70	C	381,5100098	-0,018220101	1,901450038	C	true
	75_75		384,2799988	-0,02029	3,663980007	C	*false*
	75_100	C	359,8299866	-0,0228101	2,969899893	C	true
	25_100	C	354,5	-0,022010099	1,277670026	C	true
	75_1*	I	454,3900146	0,02369	19,92329979	I	true
	50_1*	I	442,1900024	0,0242	17,63540077	I	true

GT – Real growth type; CL – Classification; ACC – Accuracy

Table 4.3 Cross validation analysis: scenarios divided into four sets for the four discriminant analysis

The classification of the cluster analysis was evaluated with the help of a regression analysis, in which the relation between the degree of compactness and the distance to the two centroids were examined. In Figure 4.4 the degree of compactness stands for the probability of being compact (high compactness) or isolated (low compactness) based on the growth coefficients and that is compared to the probability of belonging to the two clusters based on the metrics (distance to the centroids). The compactness is compared separately to the distance to both centroids shown in the two graphs. The same groups identified in Figure 4.3 can be identified in these graphs as well.

For example, group 2 containing the scenarios showing strong compact characteristics can be found on graph 1 with the longest distance to centroid one (around 120) and high compactness (120-140) at the right end of the regression line. This exact group however, on the second graph seems to be a group of outliers far located from the regression line. It is because even though based on the SLEUTH coefficients they show high compactness, based on the metrics although they are close to the compact centroid, and much closer than to the isolated centroid, they are not the closest scenarios to the compact centroid. This significantly reduces the value of the coefficient of determination calculated on the second graph. The scenarios 10-90 and 25-100 have the same level of compactness (120) but the shorter distance to the isolated centroid without the reduction in compactness results in a further location from the regression line in the first graph. All the combined scenarios have the same compactness level (70). They only differ in the distance to the centroids. In the graph of the isolated centre, the combined scenarios (except for 1-11, 1-1*) are located in mid-distance to the centre, on the two sides, close to the regression line. 1-1 and 1-1* are further from the centroid 1 but with the same compactness level which results in greater distance from the regression line. In the second graph, with medium compactness level the combined scenarios have very low distance from centroid 2: 25-25, 50-50, 75-75 and 100-100 are closer than 20, while the distance to centroid 2 from 1-1 any 1-1* is around 40. As opposed to the distance from centroid one, in the graph of centroid 2 they are located closer to the regression line showing a stronger linear relation. Only half of the isolated scenarios were identified by the cluster analysis as isolated, the rest is considered compact. In the second graph the isolated scenarios identified by the analysis are more

separable from the rest of the isolated scenarios identified as compact, since this group is the furthest located from centroid 2. 25-1 and 25-1* are mixed with the incorrectly classified isolated scenarios (isolated-compact scenarios, group 3). On the first graph the separation of the isolated and isolated-compact scenarios is more difficult. Based on both the distance and compactness, many scenarios from the two clusters show similar values.

Overall, looking at the two regression lines, it is visible that on the first graph the lone fits better to the scenarios, separating them in the middle, while in the second graph some of the combined scenarios are very far above the line (group 2) along with other compact scenarios located on this side of the line. The isolated and isolated-compact scenarios can be found on the other side of the line, a bit further spread. The coefficient of determination describes the goodness of fit in numbers. The difference is extensive between the models of the two centroids. While in case of the compact centroid (centroid 2) the observations are far spread from the regression line and R^2 does not reach 0.5, the distance to the isolated centroid (centroid 1) shows a stronger linear relation with the compactness (R^2=0,7). This is mainly due to the scenarios in group 2 as explained before.

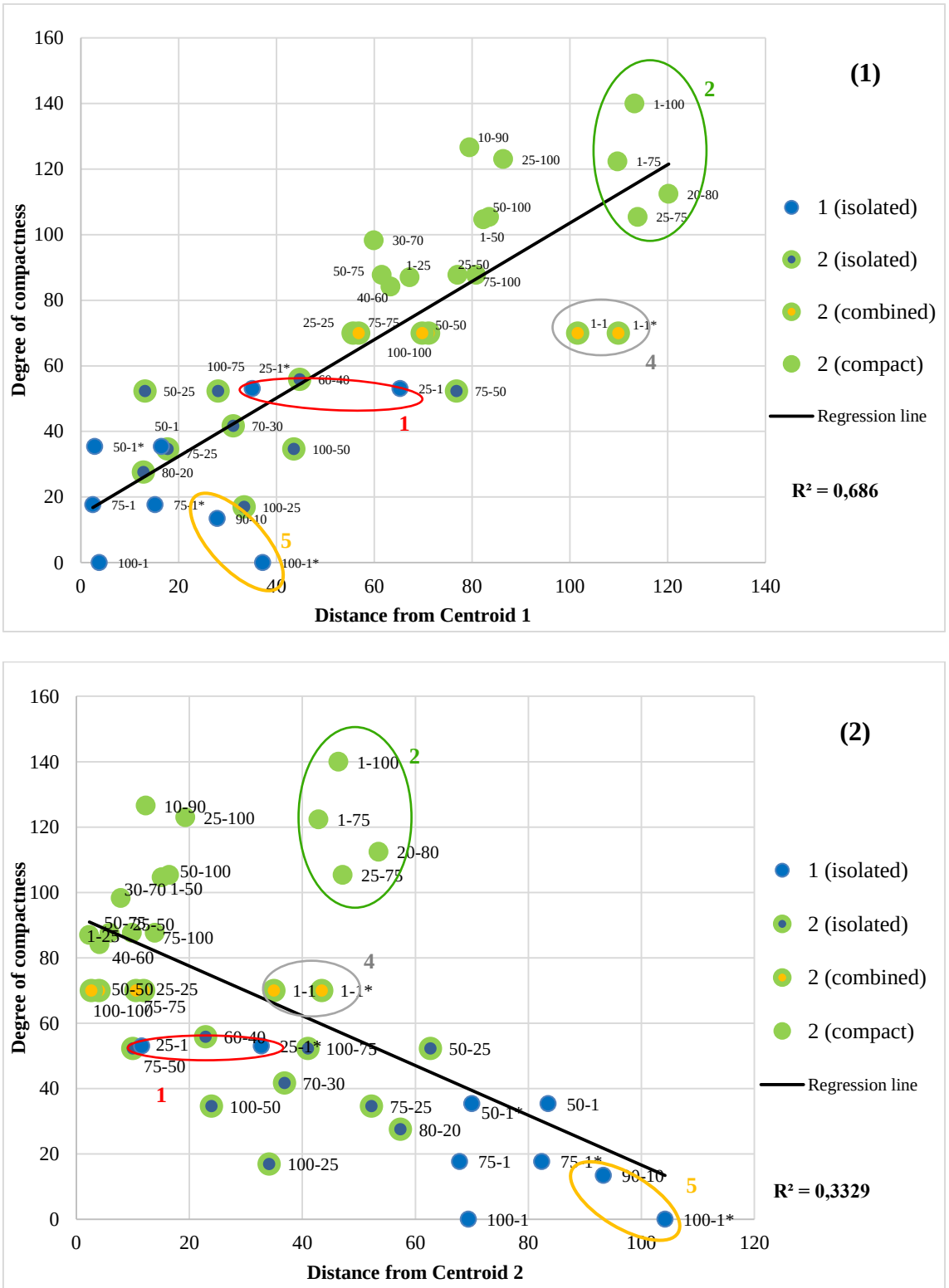

Figure 4.4 Relation between the degree of compactness and the distance to the centroids **(1)** Centroid 1 (Isolated) **(2)** Centroid 2 (Compact)

5 CONCLUSION AND RECOMMENDATION

This study presents an application of temporal and multi-temporal fragmentation metrics in the characterisation of urban growth types using simulated data. Valencia has shown dynamic urban growth in the last 30 years and the availability and consistence of the historic datasets provided a suitable database for simulation of land use change. After examining the current modelling trends of LULC change it is visible that LULC and its main driving force urbanisation is such a complex phenomenon that it is difficult to incorporate into one model all driving factors with the correct weighting. Although the SLEUTH model ignores socio-economic factors that also affect urbanisation, for the purpose of the this project it was found to be a useful instrument, predicting the changes in land use incorporating environmental drivers, such as previous changes in land use, transportation, topology and restricted areas. Besides the fact that it is freely available the most important factor was that it allows the users setting the coefficients during calibration to a certain extent. This way the scenarios could be created emphasizing certain characteristics of growth types that later could be examined with the help of the fragmentation indices.

The assessment of the metrics' suitability was conducted by applying several statistical analyses on the datasets: discriminant and cluster analysis, cross validation and regression analysis with the coefficient of determination. Looking at the results the fragmentation metrics prove to have potential in the simulated urban growth characterisation. The less growth types are distinguished the more accurate is the classification. Based on the current database the discrimination between isolated and compact growth is the most successful as they represent urban patterns with strong differences. The limitation in the classification of more growth types is a result of the similarities in the simulation of the urban pattern. The combined scenarios are a transition between two other growth types as a result they show the characteristics of

both of them, which makes it difficult to recognise them as a separate class. The metrics tend to detect the stronger influence of the spread coefficient over the diffusion when both the variables are high. The isolated and compact scenarios' classification remains highly accurate even with the third class introduced, which means that the two growth types are clearly separable from the mixed class. The coefficients used in the simulation of the road based scenarios are very similar to that of the isolated ones. This causes the confusion in the classification. Meanwhile the road based scenarios are classified with high accuracy, it reduces that of the isolated scenarios, because they show similar characteristics due to the similar SLEUTH variables used to create the scenarios. The classification using cluster analysis is more difficult, since there are no seed objects given for each cluster to help the analysis in clustering, but still it recognises the isolated scenarios showing strong isolated characteristics. The distances of the scenarios to the cluster centroids can give useful information about the compactness. The closer the scenarios are to the compact centroid and the further to the isolated their compactness is higher. The distance from the isolated scenarios characterises the compactness of the scenarios more successfully since the relation between the compactness of the scenarios and the distance to the isolated centroid is more linear than to the compact centroid.

The proposed method of including multi-temporal fragmentation indices in the characterisation and analysis of future growth can provide useful information for urban planners and enable a clearer identification of the type of growth occurring in a region in urban planning. The significance of the method lays in the capability of fast detection and categorisation of growth patterns using only LULC information, and its simple and straightforward application. However, it is important to note that the analyses were conducted on a small set of observations. A larger number of simulated scenarios are recommended to be examined to increase the accuracy of analysis and also provide scenarios for testing. Other types of urban growth could be explored and included in the study to see if more successful classification can be achieved. It could be interesting to involve other cities as well in the project to see how the metrics work in areas with different circumstances, for example more restricted areas, greater differences in topology and different size of cities.

6 REFERENCES

Allen, J. and Lu, K. (2003). Modeling and Prediction of Future Urban Growth in the Charleston Region of South Carolina: a GIS-based Integrated Approach. Conservation Ecology, 8(2).

Alsharif, A. and Pradhan, B. (2013). Urban Sprawl Analysis of Tripoli Metropolitan City (Libya) Using Remote Sensing Data and Multivariate Logistic Regression Model. Journal of the Indian Society of Remote Sensing, 42(1), pp.149-163.

Arsanjani, J. J., Helbich, M. and de Noronha Vaz, E. (2013). Spatiotemporal simulation of urban growth patterns using agent-based modeling: The case of Tehran. Cities, 32, pp.33-42.

Arsanjani, J. J., Helbich, M., Kainz, W. and Darvishi Boloorani, A. (2011). Integration of logistic regression, Markov chain and cellular automata models to simulate urban expansion. International Journal of Applied Earth Observation and Geoinformation, 21, pp.265-275.

Batty, M. and Longley, P. (1986). The Fractal Simulation of Urban Structure. Environment and Planning A, 18(9), pp.1143-1179.

Batty, M. and Longley, P. (1987). Fractal-based description of urban form. Environment and Planning B: Planning and Design, 14(2), pp.123-134.

Camagni, R., Gibelli, M. and Rigamonti, P. (2002). Urban mobility and urban form: the social and environmental costs of different patterns of urban expansion. Ecological Economics, 40(2), pp.199-216.

Candau, J. and Clarke, K. (2000). Probabilistic land cover transition modeling using deltatrons. [online] Available at:

http://www.ncgia.ucsb.edu/projects/gig/Repository/references/Santa_Barbara_CA/candau_clarke_2000.pdf [Accessed 4 May 2017].

Chaudhuri, G. and Clarke, K. (2013). The SLEUTH Land Use Change Model: A Review. The International Journal of Environmental Resources Research, 1(1).

Clarke, K. (1997). Land Transition Modeling With Deltatrons. [online] Geog.ucsb.edu. Available at: http://www.geog.ucsb.edu/~kclarke/Papers/deltatron.html [Accessed 15 May 2017].

Clarke, K. and Gaydos, L. (1998). Loose-coupling a cellular automaton model and GIS: long-term urban growth prediction for San Francisco and Washington /Baltimore. International Journal of Geographical Information Science, 12(7), pp.699-714.

Clarke, K., Hoppen, S. and Gaydos, L. (1997). A self-modifying cellular automaton model of historical urbanization in the San Francisco Bay area. Environment and Planning B: Planning and Design, 24(2), pp.247-261.

CNIG (2017). Centro de Descargas del CNIG (IGN). [online] Available at: http://centrodedescargas.cnig.es/CentroDescargas/catalogo.do#selectedSerie [Accessed 1 Jan. 2017].

Couclelis, H. (1985). Cellular Worlds: A Framework for Modeling Micro—Macro Dynamics. Environment and Planning A, 17(5), pp.585-596.

Couclelis, H. (1997). From cellular automata to urban models: new principles for model development and implementation. Environment and Planning B: Planning and Design, 24(2), pp.165-174.

Cox, D. (1958). The Regression Analysis of Binary Sequences. Journal of the Royal Statistical Society. Series B (Methodological), 20(2), pp.215-242.

Dietzel, C. and Clarke, K. (2007). Toward Optimal Calibration of the SLEUTH Land Use Change Model. Transactions in GIS, 11(1), pp.29-45.

Estivill-Castro, V. (2002). Why so many clustering algorithms. ACM SIGKDD Explorations Newsletter, 4(1), pp.65-75.

Eurostat (2017). Eurostat. [online] Available at: http://ec.europa.eu/eurostat/web/main/home [Accessed 4 Jul. 2017].

Fang, S., Gertner, G., Sun, Z. and Anderson, A. (2005). The impact of interactions in spatial simulation of the dynamics of urban sprawl. Landscape and Urban Planning, 73(4), pp.294-306.

Foley, J., DeFries, R., Asner, G., Barford, C., at al. (2005). Global Consequences of Land Use. Science, 309(5734), pp.570-574.

Fotheringham, A., Batty, M. and Longley, P. (1989). Diffusion-limited aggregation and the fractal nature of urban growth. Papers in Regional Science, 67(1), pp.55-69.

Frankhauser, P. (2008). Fractal Geometry for Measuring and Modelling Urban Patterns. In Albeverio, S. (Ed.) The dynamics of complex urban systems. pp.213-243. Heidelberg: Physica-Verlag,

Hannah, L. (2011). Climate Change, Connectivity, and Conservation Success. Conservation Biology, 25(6), pp.1139-1142.

Hu, Z. and Lo, C. (2007). Modeling urban growth in Atlanta using logistic regression. Computers, Environment and Urban Systems, 31(6), pp.667-688.

Hussain, A. and Ivanović, M. (2015). Electronics, communications and networks IV. Leiden: CRC Press/Balkema.

INE (2017). Instituto Nacional de Estadistica. (Spanish Statistical Office). [online] Available at: http://www.ine.es/en/welcome.shtml [Accessed 1 Jun. 2017].

Kanungo, D., Arora, M., Sarkar, S. and Gupta, R. (2006). A comparative study of conventional, ANN black box, fuzzy and combined neural and fuzzy weighting procedures for landslide susceptibility zonation in Darjeeling Himalayas. Engineering Geology, 85(3-4), pp.347-366.

Kamusoko, C. and Aniya, M. (2007). Land use/cover change and landscape fragmentation analysis in the Bindura District, Zimbabwe. Land Degradation & Development, 18(2), pp.221-233.

Copernicus (2017). Urban Atlas 2012 — Copernicus Land Monitoring Service. [online] Available at: http://land.copernicus.eu/local/urban-atlas/urban-atlas-2012 [Accessed 10 Jul. 2017].

Li, X. and Yeh, A. (2002). Neural-network-based cellular automata for simulating multiple land use changes using GIS. International Journal of Geographical Information Science, 16(4), pp.323-343.

Ligtenberg, A., Bregt, A. and van Lammeren, R. (2001). Multi-actor-based land use modelling: spatial planning using agents. Landscape and Urban Planning, 56(1-2), pp.21-33.

Linh, N., Erasmi, S. and Kappas, M. (2012). Quantifying land use/cover change and landscape fragmentation in danang city, vietnam: 1979-2009. ISPRS - International Archives of the Photogrammetry, Remote Sensing and Spatial Information Sciences, XXXIX-B8, pp.501-506.

Liu, X., Li, X., Chen, Y., Tan, Z., Li, S. and Ai, B. (2010). A new landscape index for quantifying urban expansion using multi-temporal remotely sensed data. Landscape Ecology, 25(5), pp.671-682.

Luck, M. and Wu, J. (2002). A gradient analysis of urban landscape pattern: a case study from the Phoenix metropolitan region, Arizona, USA. Landscape Ecology, 17, pp.327–339.

Magliocca, N., McConnell, V., Walls, M. and Safirova, E. (2012). Explaining Sprawl with an Agent-Based Model of Exurban Land and Housing Markets. SSRN Electronic Journal.

Maithani, S. (2009). A neural network based urban growth model of an Indian city. Journal of the Indian Society of Remote Sensing, 37(3), pp.363-376.

Mandelbrot, B. (1983). The fractal geometry of nature. San Francisco: W.H. Freeman.

Montgomery, D. and Runger, G. (1999). Applied statistics and probability for engineers. 2nd ed.

Moore, D., McCabe, G. and Craig, B. (2014). Introduction to the practice of statistics.

Myint, S. (2003). Fractal approaches in texture analysis and classification of remotely sensed data: Comparisons with spatial autocorrelation techniques and simple descriptive statistics. International Journal of Remote Sensing, 24(9), pp.1925-1947.

Nagendra, H., Munroe, D. and Southworth, J. (2004). From pattern to process: landscape fragmentation and the analysis of land use/land cover change. Agriculture, Ecosystems & Environment, 101(2-3), pp.111-115.

Project Gigalopolis (2017). Project Gigalopolis. [online] Available at: http://www.ncgia.ucsb.edu/projects/gig/index.html [Accessed 15 May 2017].

Park, S., Jeon, S., Kim, S. and Choi, C. (2011). Prediction and comparison of urban growth by land suitability index mapping using GIS and RS in South Korea. Landscape and Urban Planning, 99(2), pp.104-114.

Pijanowski, B., Brown, D., Shellito, B. and Manik, G. (2002). Using neural networks and GIS to forecast land use changes: a Land Transformation Model. Computers, Environment and Urban Systems, 26(6), pp.553-575.

Piqueras Haba, J. (1999). El espacio valenciano - Una síntesis geográfica. 1st ed. Valencia: Editorial Gules, S.L., pp.20-29.

Rumelhart, D., Hinton, G. and Williams, R. (1986). Learning representations by back-propagating errors. Nature, 323(6088), pp.533-536.

Santé, I., García, A., Miranda, D. and Crecente, R. (2010). Cellular automata models for the simulation of real-world urban processes: A review and analysis. Landscape and Urban Planning, 96(2), pp.108-122.

Sapena, M. and Ruiz, L. (2015a). Descripción y cálculo de índices de fragmentación urbana: Herramienta IndiFrag. Revista de Teledetección, (43), pp.77-89.

Sapena, M. and Ruiz, L. (2015b). Analysis of urban development by means of multi-temporal fragmentation metrics from LULC data. ISPRS - International Archives of the Photogrammetry, Remote Sensing and Spatial Information Sciences, XL-7/W3, pp.1411-1418.

Sede Electrónica del Catastro (2017). Sede Electrónica del Catastro. [online] Available at: https://www1.sedecatastro.gob.es/ [Accessed 10 Jul. 2017].

Shalaby, A., Ghar, M. and Tateishi, R. (2004). Desertification impact assessment in Egypt using low resolution satellite data and GIS. International Journal of Environmental Studies, 61(4), pp.375-383.

Shen, G. (2002). Fractal dimension and fractal growth of urbanized areas. International Journal of Geographical Information Science, 16(5), pp.419-437.

Silva, E. and Clarke, K. (2002). Calibration of the SLEUTH urban growth model for Lisbon and Porto, Portugal. Computers, Environment and Urban Systems, 26(6), pp.525-552.

Sun, C., Wu, Z., Lv, Z., Yao, N. and Wei, J. (2013). Quantifying different types of urban growth and the change dynamic in Guangzhou using multi-temporal remote sensing data. International Journal of Applied Earth Observation and Geoinformation, 21, pp.409-417.

Tan, P., Steinbach, M. and Kumar, V. (2015). Introduction to data mining. Dorling Kindersley: Pearson.

Tannier, C., Thomas, I., Vuidel, G. and Frankhauser, P. (2011). A Fractal Approach to Identifying Urban Boundaries. Geographical Analysis, 43(2), pp.211-227.

Tayyebi, A., Pijanowski, B. and Tayyebi, A. (2011). An urban growth boundary model using neural networks, GIS and radial parameterization: An application to Tehran, Iran. Landscape and Urban Planning, 100(1-2), pp.35-44.

Terando, A., Costanza, J., Belyea, C., Dunn, R., McKerrow, A. and Collazo, J. (2014). The Southern Megalopolis: Using the Past to Predict the Future of Urban Sprawl in the Southeast U.S. PLoS ONE, 9(7), p.e102261.

Theobald, D. (2005). Landscape Patterns of Exurban Growth in the USA from 1980 to 2020. Ecology and Society, 10(1).

Tian, G., Ma, B., Xu, X., Liu, X., Xu, L., Liu, X., Xiao, L. and Kong, L. (2016). Simulation of urban expansion and encroachment using cellular automata and multi-agent system model—A case study of Tianjin metropolitan region, China. Ecological Indicators, 70, pp.439-450.

Triantakonstantis, D. and Mountrakis, G. (2012). Urban Growth Prediction: A Review of Computational Models and Human Perceptions. Journal of Geographic Information System, 04(06), pp.555-587.

Triantakonstantis, D. (2012). Urban Growth Prediction Modelling Using Fractals and Theory of Chaos. Open Journal of Civil Engineering, 02(02), pp.81-86.

UN (2017). United Nations. url: https://esa.un.org/unpd/wup/DataQuery/ [Accessed 9 May 2017].

Weber, C. (2003). Interaction model application for urban planning. Landscape and Urban Planning, 63(1), pp.49-60.

Wilson, E., Hurd, J., Civco, D., Prisloe, M. and Arnold, C. (2003). Development of a geospatial model to quantify, describe and map urban growth. Remote Sensing of Environment, 86(3), pp.275-285.

Wolfram, S. (1984). Cellular automata as models of complexity. Nature, 311(5985), pp.419-424.

Yang, X., Chen, R. and Zheng, X. (2015). Simulating land use change by integrating ANN-CA model and landscape pattern indices. Geomatics, Natural Hazards and Risk, 7(3), pp.918-932.

Yin, J., Yin, Z., Zhong, H., Xu, S., Hu, X., Wang, J. and Wu, J. (2010). Monitoring urban expansion and land use/land cover changes of Shanghai metropolitan area during the transitional economy (1979–2009) in China. Environmental Monitoring and Assessment, 177(1-4), pp.609-621.

Yuan, F., Sawaya, K., Loeffelholz, B. and Bauer, M. (2005). Land cover classification and change analysis of the Twin Cities (Minnesota) Metropolitan Area by multitemporal Landsat remote sensing. Remote Sensing of Environment, 98(2-3), pp.317-328.

Yue, W., Liu, Y. and Fan, P. (2013). Measuring urban sprawl and its drivers in large Chinese cities: The case of Hangzhou. Land Use Policy, 31, pp.358-370.

Zhang, H., Zeng, Y., Bian, L. and Yu, X. (2010). Modelling urban expansion using a multi agent-based model in the city of Changsha. Journal of Geographical Sciences, 20(4), pp.540-556.

7 APPENDICES

APPENDIX 1

Example scenario file from the SLEUTH model used for the prediction step of the road based scenario 75-1* (Project Gigalopolis, 2017)

```
# FILE: 'scenario file' for SLEUTH land cover transition model
#       (UGM  v3.0)
#       Comments start with #
#
#   I. Path Name Variables
#  II. Running Status (Echo)
# III. Output ASCII Files
#  IV. Log File Preferences
#   V. Working Grids
#  VI. Random Number Seed
# VII. Monte Carlo Iteration
#VIII. Coefficients
#      A. Coefficients and Growth Types
#      B. Modes and Coefficient Settings
#  IX. Prediction Date Range
#   X. Input Images
#  XI. Output Images
# XII. Colortable Settings
#      A. Date_Color
#      B. Non-Landuse Colortable
#      C. Land Cover Colortable
#      D. Growth Type Images
#      E. Deltatron Images
#XIII. Self Modification Parameters

# I.PATH NAME VARIABLES
#   INPUT_DIR: relative or absolute path where input image files and
#              (if modeling land cover) 'landuse.classes' file are
#              located.
#   OUTPUT_DIR: relative or absolute path where all output files will
#               be located.
#   WHIRLGIF_BINARY: relative path to 'whirlgif' gif animation program.
#                    These must be compiled before execution.
INPUT_DIR=../Input/vlc30new/
OUTPUT_DIR=../Output/vlc30/prediction/maxvalue/roadslope0/75-75-1-1-100/
WHIRLGIF_BINARY=../Whirlgif/whirlgif

# II. RUNNING STATUS (ECHO)
#  Status of model run, monte carlo iteration, and year will be
#  printed to the screen during model execution.
ECHO(YES/NO)=yes

# III. Output Files
# INDICATE TYPES OF ASCII DATA FILES TO BE WRITTEN TO OUTPUT_DIRECTORY.
#
#   COEFF_FILE: contains coefficient values for every run, monte carlo
#               iteration and year.
#   AVG_FILE: contains measured values of simulated data averaged over
#             monte carlo iterations for every run and control year.
#   STD_DEV_FILE: contains standard diviation of averaged values
#                 in the AVG_FILE.
#   MEMORY_MAP: logs memory map to file 'memory.log'
#   LOGGING: will create a 'LOG_#' file where # signifies the processor
#            number that created the file if running code in parallel.
#            Otherwise, # will be 0. Contents of the LOG file may be
#            described below.
WRITE_COEFF_FILE(YES/NO)=yes
WRITE_AVG_FILE(YES/NO)=yes
WRITE_STD_DEV_FILE(YES/NO)=yes
WRITE_MEMORY_MAP(YES/NO)=YES
LOGGING(YES/NO)=YES

# IV. Log File Preferences
# INDICATE CONTENT OF LOG_# FILE (IF LOGGING == ON).
#   LANDCLASS_SUMMARY: (if landuse is being modeled) summary of input
#                      from 'landuse.classes' file
#   SLOPE_WEIGHTS(YES/NO): annual slope weight values as effected
#                          by slope_coeff
#   READS(YES/NO)= notes if a file is read in
#   WRITES(YES/NO)= notes if a file is written
#   COLORTABLES(YES/NO)= rgb lookup tables for all colortables generated
#   PROCESSING_STATUS(0:off/1:low verbosity/2:high verbosity)=
#   TRANSITION_MATRIX(YES/NO)= pixel count and annual probability of
#                              land class transitions
```

```
#   URBANIZATION_ATTEMPTS(YES/NO)= number of times an attempt to urbanize
#                                  a pixel occurred
#   INITIAL_COEFFICIENTS(YES/NO)= initial coefficient values for
#                                 each monte carlo
#   BASE_STATISTICS(YES/NO)= measurements of urban control year data
#   DEBUG(YES/NO)= data dump of igrid object and grid pointers
#   TIMINGS(0:off/1:low verbosity/2:high verbosity)= time spent within
#     each module. If running in parallel, LOG_0 will contain timing for
#     complete job.
LOG_LANDCLASS_SUMMARY(YES/NO)=yes
LOG_SLOPE_WEIGHTS(YES/NO)=no
LOG_READS(YES/NO)=no
LOG_WRITES(YES/NO)=no
LOG_COLORTABLES(YES/NO)=no
LOG_PROCESSING_STATUS(0:off/1:low verbosity/2:high verbosity)=1
LOG_TRANSITION_MATRIX(YES/NO)=yes
LOG_URBANIZATION_ATTEMPTS(YES/NO)=yes
LOG_INITIAL_COEFFICIENTS(YES/NO)=no
LOG_BASE_STATISTICS(YES/NO)=yes
LOG_DEBUG(YES/NO)= yes
LOG_TIMINGS(0:off/1:low verbosity/2:high verbosity)=1

# V. WORKING GRIDS
# The number of working grids needed from memory during model execution is

# designated up front. This number may change depending upon modes. If
# NUM_WORKING_GRIDS needs to be increased, the execution will be exited
# and an error message will be written to the screen and to 'ERROR_LOG'
# in the OUTPUT_DIRECTORY. If the number may be decreased an optimal
# number will be written to the end of the LOG_0 file.
NUM_WORKING_GRIDS=5

# VI. RANDOM NUMBER SEED
# This number initializes the random number generator. This seed will be
# used to initialize each model run.
RANDOM_SEED=1

# VII. MONTE CARLO ITERATIONS
# Each model run may be completed in a monte carlo fashion.
#  For CALIBRATION or TEST mode measurements of simulated data will be
#  taken for years of known data, and averaged over the number of monte
#  carlo iterations. These averages are written to the AVG_FILE, and
#  the associated standard diviation is written to the STD_DEV_FILE.
#  The averaged values are compared to the known data, and a Pearson
#  correlation coefficient measure is calculated and written to the
#  control_stats.log file. The input per run may be associated across
#  files using the 'index' number in the files' first column.
#
MONTE_CARLO_ITERATIONS=100

# VIII. COEFFICIENTS
# The coefficients effect how the growth rules are applied to the data.
# Setting requirements:
#    *_START values >= *_STOP values
#    *_STEP values > 0
#   if no coefficient increment is desired:
#    *_START == *_STOP
#    *_STEP == 1
# For additional information about how these values affect simulated
# land cover change see our publications and PROJECT GIGALOPOLIS
#  site: (www.ncgia.ucsb.edu/project/gig/About/abGrowth.htm).
#  A. COEFFICIENTS AND GROWTH TYPES
#     DIFFUSION: affects SPONTANEOUS GROWTH and search distance along the
#                road network as part of ROAD INFLUENCED GROWTH.
#     BREED: NEW SPREADING CENTER probability and affects number of ROAD
#            INFLUENCED GROWTH attempts.
#     SPREAD: the probabilty of ORGANIC GROWTH from established urban
#             pixels occuring.
#     SLOPE_RESISTANCE: affects the influence of slope to urbanization. As
#                       value increases, the ability to urbanize
#                       ever steepening slopes decreases.
#     ROAD_GRAVITY: affects the outward distance from a selected pixel for
#                   which a road pixel will be searched for as part of
#                   ROAD INFLUENCED GROWTH.
```

```
#
#  B. MODES AND COEFFICIENT SETTINGS
#     TEST: TEST mode will perform a single run through the historical
#           data using the CALIBRATION_*_START values to initialize
#           growth, complete the MONTE_CARLO_ITERATIONS, and then conclude
#           execution. GIF images of the simulated urban growth will be
#           written to the OUTPUT_DIRECTORY.
#     CALIBRATE: CALIBRATE will perform monte carlo runs through the
#                historical data using every combination of the
#                coefficient values indicated. The CALIBRATION_*_START
#                coefficient values will initialize the first run. A
#                coefficient will then be increased by its *_STEP value,
#                and another run performed. This will be repeated for all
#                possible permutations of given ranges and increments.
#     PREDICTION: PREDICTION will perform a single run, in monte carlo
#                 fashion, using the PREDICTION_*_BEST_FIT values
#                 for initialization.

CALIBRATION_DIFFUSION_START= 0
CALIBRATION_DIFFUSION_STEP=  1
CALIBRATION_DIFFUSION_STOP=  0

CALIBRATION_BREED_START=     0
CALIBRATION_BREED_STEP=      1
CALIBRATION_BREED_STOP=      0

CALIBRATION_SPREAD_START=    6
CALIBRATION_SPREAD_STEP=     1
CALIBRATION_SPREAD_STOP=     6

CALIBRATION_SLOPE_START=     0
CALIBRATION_SLOPE_STEP=      1
CALIBRATION_SLOPE_STOP=      0

CALIBRATION_ROAD_START=      0
CALIBRATION_ROAD_STEP=       1
CALIBRATION_ROAD_STOP=       0

PREDICTION_DIFFUSION_BEST_FIT= 75
PREDICTION_BREED_BEST_FIT= 75
PREDICTION_SPREAD_BEST_FIT= 1
PREDICTION_SLOPE_BEST_FIT=  1
PREDICTION_ROAD_BEST_FIT=  100

# IX. PREDICTION DATE RANGE
# The urban and road images used to initialize growth during
# prediction are those with dates equal to, or greater than,
# the PREDICTION_START_DATE. If the PREDICTION_START_DATE is greater
# than any of the urban dates, the last urban file on the list will be
# used. Similarly, if the PREDICTION_START_DATE is greater
# than any of the road dates, the last road file on the list will be
# used. The prediction run will terminate at PREDICTION_STOP_DATE.
#
PREDICTION_START_DATE=2012
PREDICTION_STOP_DATE=2100

# X. INPUT IMAGES
# The model expects grayscale, GIF image files with file name
# format as described below. For more information see our
# PROJECT GIGALOPOLIS web site:
# (www.ncgia.ucsb.edu/project/gig/About/dtInput.htm).
#
# IF LAND COVER IS NOT BEING MODELED: Remove or comment out
# the LANDUSE_DATA data input flags below.
#
#    <  >  = user selected fields
#   [<  >] = optional fields
#
# Urban data GIFs
#  format:  <location>.urban.<date>.[<user info>].gif
#
#
URBAN_DATA= vlc30.urban.1994.gif
URBAN_DATA= vlc30.urban.2000.gif
```

```
URBAN_DATA= vlc30.urban.2006.gif
URBAN_DATA= vlc30.urban.2012.gif
#
# Road data GIFs
#  format:  <location>.roads.<date>.[<user info>].gif
#
ROAD_DATA= vlc30.roads.2006.gif
ROAD_DATA= vlc30.roads.2012.gif
#
# Landuse data GIFs
#  format:  <location>.landuse.<date>.[<user info>].gif
#
LANDUSE_DATA=vlc30.landuse.2006.gif
LANDUSE_DATA= vlc30.landuse.2012.gif
#
# Excluded data GIF
#  format:  <location>.excluded.[<user info>].gif
#
EXCLUDED_DATA=vlc30.excluded.gif
#
# Slope data GIF
#  format:  <location>.slope.[<user info>].gif
#
SLOPE_DATA= vlc30.slope.gif
#
# Background data GIF
#  format:   <location>.hillshade.[<user info>].gif
#
#BACKGROUND_DATA= demo200.hillshade.gif
BACKGROUND_DATA= vlc30.hillshade.gif

# XI. OUTPUT IMAGES
#   WRITE_COLOR_KEY_IMAGES: Creates image maps of each colortable.
#                           File name format: 'key_[type]_COLORMAP'
#                           where [type] represents the colortable.
#   ECHO_IMAGE_FILES: Creates GIF of each input file used in that job.
#                     File names format: 'echo_of_[input_filename]'
#                     where [input_filename] represents the input name.
#   ANIMATION: if whirlgif has been compiled, and the WHIRLGIF_BINARY
#              path has been defined, animated gifs begining with the
#              file name 'animated' will be created in PREDICT mode.
WRITE_COLOR_KEY_IMAGES(YES/NO)=yes
ECHO_IMAGE_FILES(YES/NO)=yes
ANIMATION(YES/NO)= yes

# XII. COLORTABLE SETTINGS
#  A. DATE COLOR SETTING
#     The date will automatically be placed in the lower left corner
#     of output images. DATE_COLOR may be designated in with red, green,
#     and blue values (format: <red_value, green_value, blue_value> )
#     or with hexadecimal begining with '0X' (format: <0X######> ).
#default DATE_COLOR= 0XFFFFFF white
DATE_COLOR=     0XFFFFFF #white

#  B. URBAN (NON-LANDUSE) COLORTABLE SETTINGS
#     1. URBAN MODE OUTPUTS
#         TEST mode: Annual images of simulated urban growth will be
#                    created using SEED_COLOR to indicate urbanized areas.

#         CALIBRATE mode: Images will not be created.
#         PREDICT mode: Annual probability images of simulated urban
#                       growth will be created using the PROBABILITY
#                       _COLORTABLE. The initializing urban data will be
#                       indicated by SEED_COLOR.
#
#     2. COLORTABLE SETTINGS
#          SEED_COLOR: initializing and extrapolated historic urban extent

#          WATER_COLOR: BACKGROUND_DATA is used as a backdrop for

#                       simulated urban growth. If pixels in this file
#                       contain the value zero (0), they will be filled
#                       with the color value in WATER_COLOR. In this way,
#                       major water bodies in a study area may be included
```

```
#                       in output images.
#SEED_COLOR= 0XFFFF00 #yellow
SEED_COLOR=  249, 209, 110 #pale yellow
#WATER_COLOR=  0X0000FF # blue
WATER_COLOR=  20, 52, 214 # royal blue

#     3. PROBABILITY COLORTABLE FOR URBAN GROWTH
#        For PREDICTION, annual probability images of urban growth
#        will be created using the monte carlo iterations. In these
#        images, the higher the value the more likely urbanizaion is.
#        In order to interpret these 'continuous' values more easily
#        they may be color classified by range.
#
#        If 'hex' is not present then the range is transparent.
#        The transparent range must be the first on the list.
#        The max number of entries is 100.
#          PROBABILITY_COLOR: a color value in hexadecimal that indicates
#                             a probability range.
#            low/upper: indicate the boundaries of the range.
#
#                  low,  upper,   hex,  (Optional Name)
PROBABILITY_COLOR=   0,    50,         , #transparent
PROBABILITY_COLOR=   50,   60, 0X005A00, #0, 90,0 dark green
PROBABILITY_COLOR=   60,   70, 0X008200, #0,130,0
PROBABILITY_COLOR=   70,   80, 0X00AA00, #0,170,0
PROBABILITY_COLOR=   80,   90, 0X00D200, #0,210,0
PROBABILITY_COLOR=   90,   95, 0X00FF00, #0,255,0 light green
PROBABILITY_COLOR=   95,  100, 0X8B0000, #dark red

#  C. LAND COVER COLORTABLE
#  Land cover input images should be in grayscale GIF image format.
#  The 'pix' value indicates a land class grayscale pixel value in
#  the image. If desired, the model will create color classified
#  land cover output. The output colortable is designated by the
#  'hex/rgb' values.
#    pix: input land class pixel value
#    name: text string indicating land class
#    flag: special case land classes
#          URB - urban class (area is included in urban input data
#                and will not be transitioned by deltatron)
#          UNC - unclass (NODATA areas in image)
#          EXC - excluded (land class will be ignored by deltatron)
#    hex/rgb: hexidecimal or rgb (red, green, blue) output colors
#
#              pix, name,     flag,   hex/rgb, #comment
LANDUSE_CLASS=  0,  Unclass , UNC   , 0X000000
LANDUSE_CLASS=  1,  Urban   , URB   , 0X8b2323 #dark red
LANDUSE_CLASS=  2,  Agric   ,       , 0Xffec8b #pale yellow
LANDUSE_CLASS=  3,  Range   ,       , 0Xee9a49 #tan
LANDUSE_CLASS=  4,  Forest  , EXC   , 0X006400
LANDUSE_CLASS=  5,  Water   ,       , 0X104e8b
LANDUSE_CLASS=  6,  Wetland ,       , 0X483d8b
LANDUSE_CLASS=  7,  Barren  ,       , 0Xeec591

#  D. GROWTH TYPE IMAGE OUTPUT CONTROL AND COLORTABLE
#
#  From here you can control the output of the Z grid
#  (urban growth) just after it is returned from the spr_spread()
#  function. In this way it is possible to see the different types
#  of growth that have occured for a particular growth cycle.
#
#  VIEW_GROWTH_TYPES(YES/NO) provides an on/off
#  toggle to control whether the images are generated.
#
#  GROWTH_TYPE_PRINT_WINDOW provides a print window
#  to control the amount of images created.
#  format:  <start_run>,<end_run>,<start_monte_carlo>,
#           <end_monte_carlo>,<start_year>,<end_year>
#  for example:
#  GROWTH_TYPE_PRINT_WINDOW=run1,run2,mc1,mc2,year1,year2
#  so images are only created when
#  run1<= current run <=run2 AND
#  mc1 <= current monte carlo <= mc2 AND
#  year1 <= currrent year <= year2
```

```
#
#  0 == first
VIEW_GROWTH_TYPES(YES/NO)=yes
GROWTH_TYPE_PRINT_WINDOW=0,0,0,0,2012,2100
PHASE0G_GROWTH_COLOR=  0xff0000 # seed urban area
PHASE1G_GROWTH_COLOR=  0X00ff00 # diffusion growth
PHASE2G_GROWTH_COLOR=  0X0000ff # NOT USED
PHASE3G_GROWTH_COLOR=  0Xffff00 # breed growth
PHASE4G_GROWTH_COLOR=  0Xffffff # spread growth
PHASE5G_GROWTH_COLOR=  0X00ffff # road influenced growth

#************************************************************
#
#  E. DELTATRON AGING SECTION
#
#  From here you can control the output of the deltatron grid
#  just before they are aged
#
#  VIEW_DELTATRON_AGING(YES/NO) provides an on/off
#  toggle to control whether the images are generated.
#
#  DELTATRON_PRINT_WINDOW provides a print window
#  to control the amount of images created.
#  format:  <start_run>,<end_run>,<start_monte_carlo>,
#           <end_monte_carlo>,<start_year>,<end_year>
#  for example:
#  DELTATRON_PRINT_WINDOW=run1,run2,mc1,mc2,year1,year2
#  so images are only created when
#  run1<= current run <=run2 AND
#  mc1 <= current monte carlo <= mc2 AND
#  year1 <= currrent year <= year2
#
#  0 == first
VIEW_DELTATRON_AGING(YES/NO)=NO
DELTATRON_PRINT_WINDOW=0,0,0,0,1930,2020
DELTATRON_COLOR=  0x000000 # index 0 No or dead deltatron
DELTATRON_COLOR=  0X00FF00 # index 1 age = 1 year
DELTATRON_COLOR=  0X00D200 # index 2 age = 2 year
DELTATRON_COLOR=  0X00AA00 # index 3 age = 3 year
DELTATRON_COLOR=  0X008200 # index 4 age = 4 year
DELTATRON_COLOR=  0X005A00 # index 5 age = 5 year

# XIII. SELF-MODIFICATION PARAMETERS
#       SLEUTH is a self-modifying cellular automata. For more
#       information see our PROJECT GIGALOPOLIS web site
#       (www.ncgia.ucsb.edu/project/gig/About/abGrowth.htm)
#       and publications (and/or grep 'self modification' in code).
ROAD_GRAV_SENSITIVITY=0.0001
SLOPE_SENSITIVITY=0.0001
CRITICAL_LOW=1
CRITICAL_HIGH=1
CRITICAL_SLOPE=21.0
BOOM=1
BUST=1
```

APPENDIX 2

Examples of output scenarios of the SLEUTH model from each growth type:

Isolated (50-1)

Compact (1-50)

Combined (50-50)

Road based (50-1*)

Isolated (50-1)

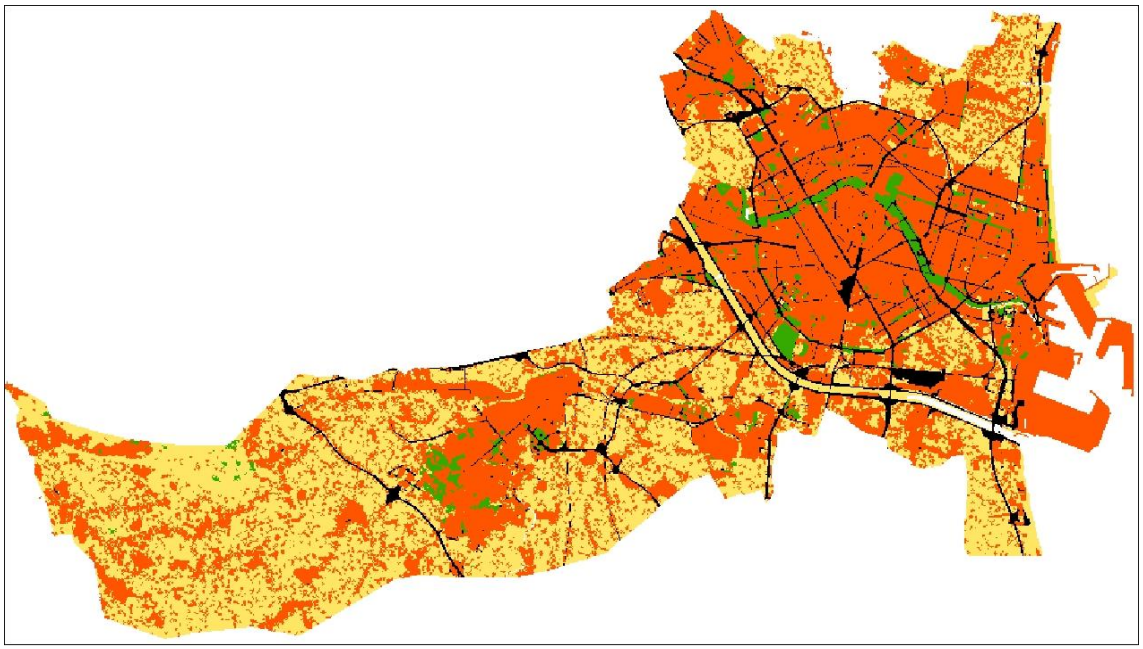

Compact (1-50)

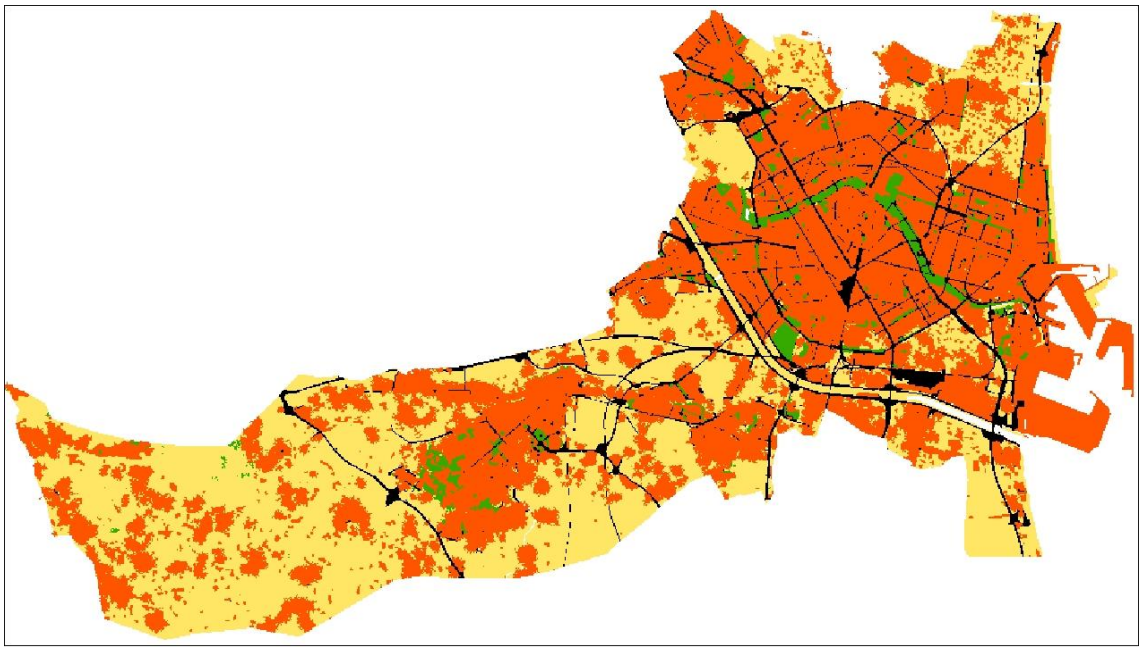

Urban	Agricultural	Green area	Road

Combined (50-50)

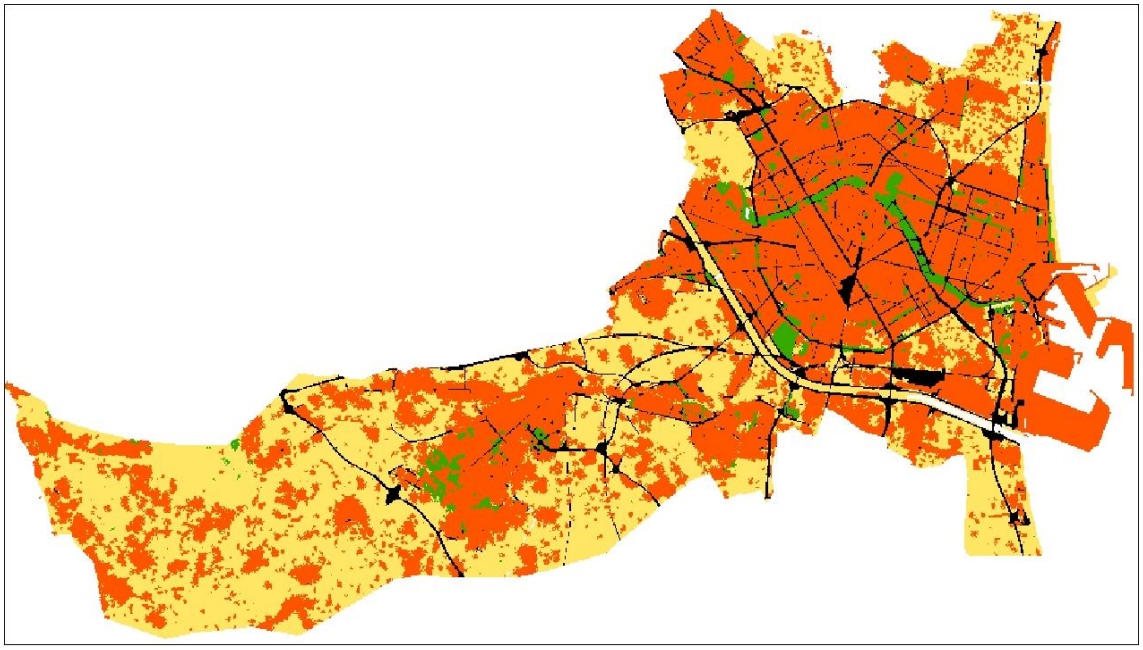

Road based (50-1*)

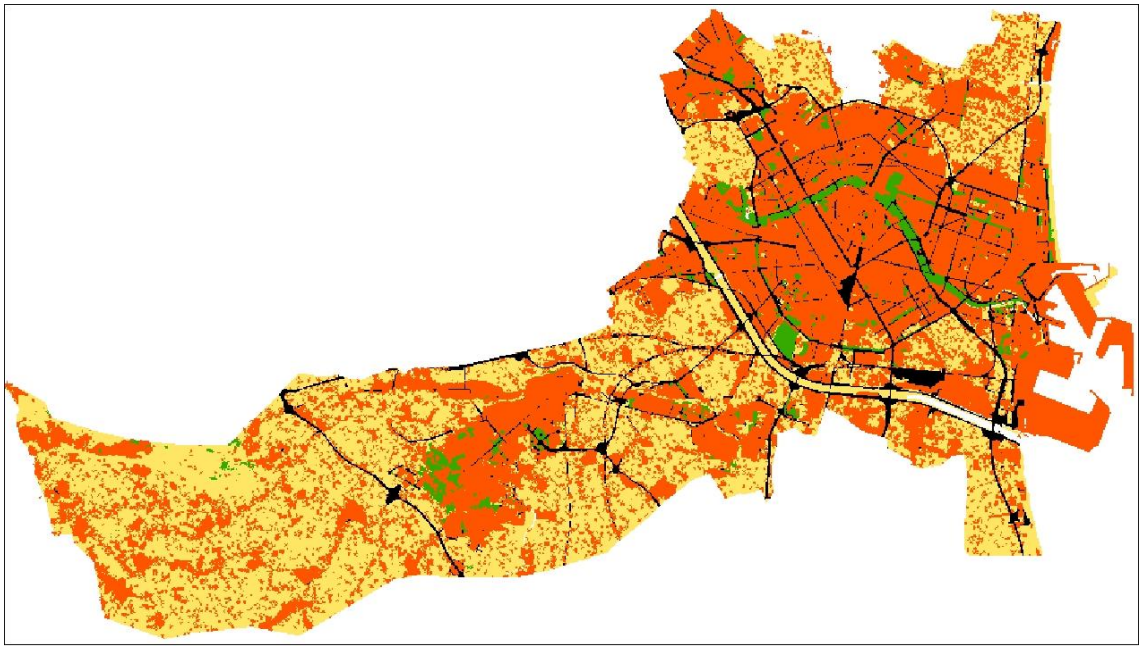

Urban	Agricultural	Green area	Road

APPENDIX 3

List of all temporal and multi-temporal fragmentation metrics with the hierarchical levels and the elimination step

		Metrics		Hierarchy	
				SO	Cl
Temporal	Area and Perimeter	DB	Edge Density	**1**	**1**
		DC	Class Density		0
		DU	Urban Density	0	
		TM	Object Mean Size	**1**	**1**
		DimB	Boundary Dimension		**3**
		LPF	Leapfrog		**2**
		Area	Area	0	0
		Perim	Perimeter	0	**1**
		PerimT	Total Perimeter	**1**	
	Aggregation	DO	Object Density	**1**	**3**
		DEP	Weighted Standard Distance	**1**	**3**
		TEM	Effective Mesh Size	**2**	**1**
		GC	Coherence Degree	**1**	0
		IS	Splitting Index	**1**	0
		COHE	Cohesion	**1**	0
		DEM	Euclidean Nearest Neighbour Mean		**1**
		CU	Urban Compactness	0	
		CC	Class Compactness		**1**
		DimR	Radius Dimension		**2**
		Nob	Number of Objects	**1**	**1**
	Contrast	RCB	Contrast Ratio	**1**	**1**
	Diversity	DSHAN	Shannon's Diversity	**2**	
		USHAN	Shannon's Evenness	0	
		IFFR	Relative Functional Fragmentation	0	
		IFFA	Absolute Functional Fragmentation	0	
		DD	Density-Diversity	**2**	0
		SIMP	Simpson Diversity	0	
		NCl	Number of Classes	0	
	Shape	DFP	Area Weighted Mean Fractal Dimension		**2**
		DF	Fractal Dimension	0	0
		IF	Shape Index	0	0
		RMPA	Perimeter-Area Mean Ratio	0	**1**
Multi-temporal		Ainf	Infilling Area		**1**
		RC	Change Rate of Urban Expansion		0
		MEI	Mean Expansion Index		**1**
		At1	Area of class in the first time		0
		At2	Area of a class in the second time		0
		Anew	Area new		0
		Aedg	Area Edge Expansion		**2**
		Aout	Area outlying		**1**
		AWM	Area Weighted Mean		**1**
		CP	Change Proportion		0
		Ac	Change area		0
		Ar	Change area ratio		0

Hierarchy: SO – Super object; Cl – Class
Elimination of metrics:
0 – All metrics applied to the scenarios
1 – After first elimination of redundant metrics
2 – After elimination of correlating metrics
3 – Metrics used for the final analyses

APPENDIX 4

The fragmentation and multi-temporal indices calculated with IndiFrag for each scenario

SLEUTH	Area	Perim	RCB	PerimT	NCl	Nob	DU	TM	DB	RMPA	IF	DF
1_1	0,283004999	0,779999018	0,011846	229,8899994	0	1885	0,110771	-18594,5	0,00131225	0,020179201	-0,099749997	-0,0155699
1_25	0,305999994	-1,019999981	0,00275099	36,21009827	0	1071	0,111515999	-12480,7002	0,00019214	0,0185192	-0,097669996	-0,0148799
1_50	0,300002992	-0,540009022	0,00121003	14,76000023	0	956	0,110632002	-11432,2998	6,855E-05	0,0178992	-0,091820002	-0,01412
1_75	0,296005011	0,119994998	0,000560045	10,4701004	0	869	0,107359998	-10601,2002	4,40199E-05	0,017531199	-0,088969901	-0,01368
1_100	0,307007015	-0,480010986	0,000325024	0,600098014	0	887	0,106468	-10773,40039	-1,36495E-05	0,0177272	-0,093500003	-0,01428
25_1	0,261992991	3,539989948	0,028654	708,2700195	0	4200	0,111110002	-28762,59961	0,00407755	0,0207962	-0,1052	-0,01539
50_1	0,246994004	4,379990101	0,031668998	823,6199951	0	4725	0,111111	-30258	0,00474515	0,0206472	-0,109250002	-0,0155699
75_1	0,261992991	3,659990072	0,033647001	886,0200195	0	5063	0,111146003	-31119	0,00510445	0,020769199	-0,109959997	-0,01548
100_1	0,261992991	4,139999866	0,034290999	917,8499756	0	5294	0,110062003	-31669,69922	0,00528835	0,0209282	-0,111220002	-0,015699999
1_1*	0,287003011	1,259989977	0,011963	237,7799988	0	1881	0,110724002	-18568,40039	0,00135765	0,0198722	-0,099160001	-0,01534
25_1*	0,266005993	3,239989996	0,028674001	704,789978	0	4131	0,111294001	-28550,09961	0,00405705	0,020791201	-0,108280003	-0,015769999
50_1*	0,264007986	3,839999914	0,031518999	810,4799805	0	4650	0,110930003	-30054,5	0,00466785	0,020968201	-0,110600002	-0,015860001
75_1*	0,264007986	3,420000076	0,033443999	874,7999878	0	5047	0,110633999	-31079,40039	0,00503945	0,0208032	-0,109679997	-0,01554
100_1*	0,264007986	3,480000019	0,034584001	919,3200073	0	5096	0,111714996	-31199,19922	0,00529665	0,0206642	-0,107009999	-0,01509
100_100	0,309998006	-0,540009022	0,00854599	147,9900055	0	1415	0,108393997	-15316,7998	0,00083755	0,0182922	-0,092910103	-0,01425
100_25	0,28500399	1,319990039	0,018832	397,5599976	0	2439	0,113182999	-21767,80078	0,00228075	0,019691201	-0,095199898	-0,01457
100_50	0,307007015	-0,360000998	0,014453	273,7799988	0	2024	0,113032997	-19447,80078	0,00156425	0,019251199	-0,099880002	-0,0150499
100_75	0,298996001	0	0,011572	215,3699951	0	1756	0,118298002	-17753,30078	0,00122735	0,019119199	-0,097170003	-0,01482
25_100	0,304001004	-1,260010004	0,003627	49,04999924	0	1042	0,113517001	-12221,59961	0,00026641	0,017740199	-0,090599999	-0,01389
25_25	0,302994013	-0,720000982	0,00926805	160,2899933	0	1527	0,112204999	-16155,40039	0,00090905	0,019189199	-0,098949999	-0,01515
25_50	0,298996001	-0,120010003	0,006154	106,7099991	0	1355	0,112946004	-14854,2998	0,00059975	0,0190532	-0,097889997	-0,015
25_75	0,304001004	-0,360000998	0,00481004	79,4701004	0	1226	0,101758003	-13812,2998	0,00044215	0,018195201	-0,094589897	-0,01447
50_100	0,311996013	-0,66000402	0,00530404	85,35009766	0	1190	0,118775003	-13509,5	0,000475651	0,018514199	-0,093529902	-0,01448
50_25	0,302994013	0,959990978	0,013988	278,6099854	0	1968	0,109002002	-19108,40039	0,00159245	0,0194482	-0,09708	-0,0148699
50_50	0,298996001	-0,300002992	0,00989699	177,5099945	0	1607	0,111120999	-16731,09961	0,00100875	0,0190992	-0,096139997	-0,01475
50_75	0,307007015	0,0599976	0,00726604	129,6600037	0	1423	0,106936	-15378,40039	0,00073185	0,018808199	-0,09606	-0,01472
75_100	0,307007015	-0,120010003	0,00744003	131,0700073	0	1439	0,104075998	-15500	0,000739951	0,018476199	-0,096779898	-0,01465
75_25	0,283004999	0,83999598	0,016851	343,2900085	0	2300	0,111331999	-21030,40039	0,00196735	0,019651201	-0,101350002	-0,01537
75_50	0,29400599	0,599991024	0,010854	207,0599976	0	1687	0,105259001	-17288,5	0,00117975	0,018390199	-0,093549997	-0,01419
75_75	0,289992988	0,720000982	0,00892001	169,0500031	0	1610	0,111233003	-16753,90039	0,00096035	0,0190922	-0,099069998	-0,01493
10_90	0,311996013	-0,840012014	0,00158203	18,03000069	0	1006	0,114335001	-11892,7998	8,67806E-05	0,018793199	-0,09623	-0,01484
20_80	0,307007015	-1,080000043	0,00373	52,71009827	0	1081	0,106158003	-12569,2002	0,00028739	0,0182152	-0,092589997	-0,0141799
30_70	0,305007994	-0,540009022	0,00545901	89,43009949	0	1250	0,111117996	-14010,2002	0,00049955	0,0182862	-0,094439998	-0,01442
40_60	0,300994992	0,539992988	0,00656003	121,3199997	0	1393	0,111014001	-15149,59961	0,00068405	0,018654199	-0,097120002	-0,01477
60_40	0,307999015	-0,41999799	0,012695	234,5099945	0	1849	0,112843998	-18360	0,00133735	0,019026199	-0,096199997	-0,01456
70_30	0,296997011	-0,120010003	0,015554	301,5599976	0	2158	0,108792	-20235,90039	0,00172545	0,0198342	-0,10001	-0,01529
80_20	0,287993997	1,019989967	0,018906999	395,7900085	0	2570	0,109837003	-22430,90039	0,00227035	0,0200592	-0,102839999	-0,01552
90_10	0,264999002	2,279999971	0,025519	593,0100098	0	3436	0,111291997	-26175,30078	0,00341135	0,0209492	-0,104900002	-0,015699999

SLEUTH	DO	DEP	TEM	GC	IS	COHE	CU	DSHAN	USHAN	IFFR	IFFA	DD
1_1	10,85770035	57,06010056	-2989730	-0,0173508	11	-0,005	-0,0031927	-0,037505001	-0,027053	0	-0,0065284	-0,078900002
1_25	6,15199995	29,32029915	-1082850	-0,0063405	3,1	0,0006	0,000526201	-0,034805998	-0,025106	0	-0,0015234	-0,0817701
1_50	5,488500118	31,66020012	-1171350	-0,0068504	3,4	-4E-04	0,0008313	-0,035571001	-0,025658	0	-0,0006705	-0,078370102
1_75	4,986599922	20,11039925	-798450	-0,0046953	2,2	0,0013	0,0009341	-0,033762001	-0,024352999	0	-0,000310298	-0,06566
1_100	5,088900089	23,49020004	-861630	-0,0050632	2,4	0,001	0,001069	-0,033481002	-0,024150001	0	-0,0001802	-0,06216
25_1	24,23660088	60,36040115	-2743950	-0,0159269	10	-0,008	-0,0080116	-0,034596998	-0,024955999	0	-0,0156541	-0,080210097
50_1	27,27370071	45,59030151	-2129930	-0,0123763	7,1	-0,004	-0,0088026	-0,033753999	-0,024347	0	-0,0172743	-0,080210097
75_1	29,22260094	41,34030151	-2284480	-0,0132723	7,8	-0,004	-0,009233	-0,033131	-0,023898	0	-0,0183345	-0,080349997
100_1	30,55699921	50,06010056	-2424930	-0,0140839	8,4	-0,005	-0,0094222	-0,032862	-0,023703	0	-0,018679099	-0,076170102
1_1*	10,83399963	32,45999908	-1427330	-0,0083258	4,3	-0,001	-0,0033227	-0,037117001	-0,026773	0	-0,0065926	-0,0787201
25_1*	23,83679962	41,20999908	-2161890	-0,0125649	7,2	-0,004	-0,0079508	-0,035328999	-0,025482999	0	-0,015665101	-0,080920003
50_1*	26,83580017	46,17039871	-2156520	-0,0125335	7,2	-0,004	-0,0086921	-0,032650001	-0,023553001	0	-0,017193999	-0,079520002
75_1*	29,12940025	65,13040161	-3085530	-0,0179009	12	-0,007	-0,0091351	-0,031860001	-0,022978	0	-0,0182258	-0,078380004
100_1*	29,41250038	48,64009857	-2358450	-0,0137002	8,1	-0,004	-0,0093655	-0,03101	-0,022369999	0	-0,0188361	-0,082539998
100_100	8,138299942	29,09029961	-1228130	-0,0071807	3,6	0	-0,0014422	-0,033339001	-0,024048001	0	-0,0047179	-0,069689997
100_25	14,05770016	35,16019821	-1665180	-0,0096994	5,1	-0,001	-0,004687	-0,035069998	-0,025296999	0	-0,0103412	-0,088170096
100_50	11,65629959	35,99020004	-1411130	-0,0082371	4,2	-7E-04	-0,0031765	-0,034122001	-0,024613	0	-0,0079545	-0,087590002
100_75	10,1097002	39,74020004	-1564490	-0,0091211	4,8	-0,001	-0,0022329	-0,035725001	-0,025769001	0	-0,0063786	-0,107519999
25_100	5,984799862	27,20019913	-1095040	-0,0064105	3,1	0,0004	0,000208801	-0,035174001	-0,025371	0	-0,0020078	-0,089440003
25_25	8,786299706	25,74020004	-1164540	-0,0068117	3,4	0,0007	-0,0016015	-0,035158999	-0,025361	0	-0,0051145	-0,0844201
25_50	7,793499947	25,74020004	-1146620	-0,0067071	3,3	1E-04	-0,0006713	-0,035904001	-0,025898	0	-0,0034015	-0,08726
25_75	7,047599792	33,92039871	-1133880	-0,0066348	3,3	-5E-04	-0,0003882	-0,03187	-0,022985	0	-0,0026605	-0,043510102
50_100	6,838399887	27,28030014	-1062790	-0,0062262	3	0,0003	-0,0003344	-0,037308	-0,026911	0	-0,0029335	-0,109300002
50_25	11,33370018	37,15039825	-1521120	-0,0088714	4,6	-2E-04	-0,0032721	-0,033185001	-0,023937	0	-0,0077006	-0,072059996
50_50	9,249199867	28,95999908	-1212880	-0,0070898	3,5	-2E-04	-0,0018542	-0,035238001	-0,025418	0	-0,0054601	-0,080250002
50_75	8,184900284	34,8003006	-1291670	-0,0075471	3,8	-4E-04	-0,0011289	-0,032639999	-0,023544	0	-0,0040143	-0,064000003
75_100	8,277299881	29,83009911	-1171400	-0,0068524	3,4	1E-04	-0,0011868	-0,031479999	-0,022709001	0	-0,0041101	-0,052730098
75_25	13,25510025	38,25	-1621010	-0,0094439	5	-1E-03	-0,00403	-0,032910999	-0,023739001	0	-0,0092627	-0,081070103
75_50	9,712100029	35,61040115	-1326310	-0,007744	3,9	-5E-04	-0,0023129	-0,032269999	-0,023279	0	-0,0059852	-0,057410002
75_75	9,267900467	31,97999954	-1311580	-0,0076581	3,9	1E-04	-0,0016406	-0,034060001	-0,024568001	0	-0,0049236	-0,080689996
10_90	5,775599957	24,42040062	-999150	-0,0058586	2,8	0,0005	0,0008051	-0,036531001	-0,026350999	0	-0,000876699	-0,092560098
20_80	6,209599972	24,11039925	-931620	-0,0054672	2,6	0,0005	0,000187501	-0,032710001	-0,023598	0	-0,0020645	-0,06095
30_70	7,186100006	34,93019867	-1302450	-0,0076087	3,8	-2E-04	-0,0003931	-0,034242999	-0,024700001	0	-0,0030185	-0,080239996
40_60	8,012599945	33,72019958	-1219290	-0,0071275	3,5	-2E-04	-0,0009745	-0,034871001	-0,025153	0	-0,0036252	-0,079840101
60_40	10,64540005	38,58010101	-1505550	-0,0087827	4,6	-0,001	-0,0026483	-0,033976998	-0,024507999	0	-0,0069933	-0,086870097
70_30	12,43229961	40,09030151	-1629760	-0,0094975	5	-0,002	-0,0035983	-0,033156	-0,023916001	0	-0,0085554	-0,071240097
80_20	14,81400013	40,75	-1715970	-0,0099934	5,3	-0,001	-0,0047317	-0,033431001	-0,024114	0	-0,010382	-0,075300001
90_10	19,82169914	44,06010056	-1947530	-0,0113263	6,3	-0,002	-0,0067076	-0,03241	-0,023378	0	-0,0139645	-0,080910102

SLEUTH	SIMP	Area_U	Perim_U	Nob_U	LPF_U	TM_U	DB_U	RMPA_U	IF_U	DF_U	DFP_U	DC_U
1_1	-0,015144	19,28790092	366,3599854	590	-0	-12594	0,00210494	0,032471899	-0,099830002	-0,0185901	0,032919999	0,110771
1_25	-0,014235	19,42830086	131,1600037	161	-0	7263,6	0,00074522	0,027541099	-0,097460002	-0,0180501	0,019200001	0,111515999
1_50	-0,014356	19,27260017	113,6999969	108	-0	10608	0,00064461	0,02647	-0,090930097	-0,01721	0,01904	0,110632002
1_75	-0,013287	18,7038002	104,0400009	103	-0	10448	0,000589	0,025679899	-0,088940002	-0,0166	0,0195299	0,107359998
1_100	-0,013055	18,55529976	95,94010162	80	-0	11929	0,0005417	0,0250639	-0,089310102	-0,0168301	0,01859	0,106468
25_1	-0,014245	19,3355999	833,5800171	2552	-0	-42514	0,00480544	0,037793402	-0,155330002	-0,02195	0,0211899	0,111110002
50_1	-0,013973	19,32839966	937,8599854	3150	-0	-46046	0,00540904	0,0387544	-0,166449994	-0,02282	0,0159899	0,111111
75_1	-0,013751	19,34189987	999,4199829	3488	-0	-47625	0,00576364	0,039138399	-0,170619994	-0,02302	0,0169599	0,111146003
100_1	-0,013463	19,15469933	1025,160034	3673	-0	-48434	0,00591224	0,039680399	-0,174339995	-0,02356	0,0130899	0,110062003
1_1*	-0,014977	19,28160095	376,0799866	638	-0	-14173	0,00216091	0,032956202	-0,104029998	-0,0190101	0,03449	0,110724002
25_1*	-0,014498	19,36980057	826,3800049	2553	-0	-42511	0,00476354	0,038071401	-0,158659995	-0,0224301	0,0233899	0,111294001
50_1*	-0,013574	19,30590057	922,3800049	3054	-0	-45555	0,00531834	0,038643401	-0,165130004	-0,02265	0,017319901	0,110930003
75_1*	-0,013286	19,25460052	984,0599976	3450	-0	-47479	0,00567474	0,0388094	-0,168410003	-0,02276	0,00987995	0,110633999
100_1*	-0,013141	19,44179916	1020,299988	3560	-0	-47910	0,00588404	0,038652401	-0,167359993	-0,0223	0,01078	0,111714996
100_100	-0,013305	18,89010048	242,2799988	545	-0	-11284	0,00138684	0,0307645	-0,1149	-0,0190101	0,016580001	0,108393997
100_25	-0,014582	19,70639992	490,5599976	1255	-0	-28327	0,00282233	0,035253402	-0,130040005	-0,02018	0,020029901	0,113182999
100_50	-0,014254	19,69199944	368,7600098	945	-0	-22223	0,00211753	0,0334372	-0,132049993	-0,02064	0,0166	0,113032997
100_75	-0,015647	20,5991993	308,9400024	719	-0	-15879	0,00177241	0,032547802	-0,12274	-0,0198101	0,01613	0,118298002
25_100	-0,014692	19,77389908	151,1999969	223	-0	3842,9	0,00086105	0,0279854	-0,09956	-0,0178801	0,019699899	0,113517001
25_25	-0,014473	19,5461998	257,9400024	498	-0	-9128	0,00147765	0,032043502	-0,11609	-0,0199001	0,025679899	0,112204999
25_50	-0,0148	19,67219925	201,1199951	337	-0	-2175	0,00114965	0,029146999	-0,101559997	-0,01792	0,021899899	0,112946004
25_75	-0,011928	17,73810005	169,0800018	322	-0	-2887	0,00096433	0,0293958	-0,104369998	-0,0185601	0,017769899	0,101758003
50_100	-0,016198	20,68829918	189,2400055	326	-0	-893,9	0,0010804	0,029155901	-0,10531	-0,0182301	0,019689901	0,118775003
50_25	-0,013382	18,99180031	369,6600037	838	-0	-20018	0,00212296	0,032731399	-0,117919996	-0,01921	0,0210099	0,109002002
50_50	-0,01432	19,35630035	272,8800049	540	-0	-10807	0,00156417	0,0304754	-0,104139999	-0,01775	0,019400001	0,111120999
50_75	-0,012882	18,63629913	220,5599976	485	-0	-9231	0,00126152	0,030918799	-0,1127	-0,01917	0,01578	0,106936
75_100	-0,012142	18,1413002	220,0800018	516	-0	-10718	0,00125874	0,0296837	-0,118450001	-0,01907	0,0179199	0,104075998
75_25	-0,013635	19,38509941	432,4200134	1054	-0	-24727	0,00248656	0,033599701	-0,126780003	-0,0200601	0,019589899	0,111331999
75_50	-0,012508	18,33930016	295,0799866	697	-0	-16536	0,00169263	0,031116201	-0,114139996	-0,0184101	0,01605	0,105259001
75_75	-0,013958	19,3715992	259,019989	636	-0	-14055	0,0014845	0,031520799	-0,123360001	-0,01958	0,0169899	0,111233003
10_90	-0,015215	19,91970062	119,9400024	168	-0	7238,8	0,00068013	0,0281379	-0,101340003	-0,01842	0,01809	0,114335001
20_80	-0,01279	18,50130081	142,5599976	222	-0	2879,3	0,00081102	0,027772101	-0,097060099	-0,0172601	0,019069901	0,106158003
30_70	-0,013998	19,35899925	182,2200012	331	-0	-2119	0,00104019	0,028672099	-0,103880003	-0,0181201	0,017960001	0,111117996
40_60	-0,014175	19,33919907	216,7799988	442	-0	-7054	0,00123998	0,029792299	-0,109180003	-0,01851	0,015769999	0,111014001
60_40	-0,014187	19,33919907	216,7799988	442	-0	-7054	1585,98999	0,029792299	-0,109180003	-0,01851	0,015769999	97981,60156
70_30	-0,01331	19,33919907	216,7799988	442	-0	-7054	1585,98999	0,029792299	-0,109180003	-0,01851	0,015769999	97981,60156
80_20	-0,013596	19,12859917	488,8800049	1389	-0	-30723	0,00281247	0,035800401	-0,143739998	-0,0217501	0,017079899	0,109837003
90_10	-0,013436	19,3689003	682,3800049	2034	-0	-38328	0,00393164	0,037701402	-0,149379998	-0,0218201	0,0182699	0,111291997

SLEUTH	C_U	DO_U	DEP_U	DEM_U	TEM_U	GC_U	IS_U	COHE_U	DD_U	RCB_U	DimB_U	DimR_U
1_1	-0,0031927	3,398639917	338,75	-28,7677002	1403980	0,00809452	-46,00880051	0,0187988	0,186139002	0,00394505	0,021229999	0,068429902
1_25	0,000526201	0,919470012	374,1700134	-19,8586998	1497530	0,00863252	-47,63629913	0,024299599	0,186139002	-0,00456995	-0,0197201	0,069209903
1_50	0,0008313	0,613539994	358,7900085	-18,74220085	1625530	0,00937242	-49,7254982	0,025993301	0,186139002	-0,005633	-0,0244601	0,067670003
1_75	0,0009341	0,584829986	330,8999939	-19,44639969	1696030	0,00978022	-50,80939865	0,0266953	0,186139002	-0,00604296	-0,024620101	0,065669999
1_100	0,001069	0,451539993	327,3900146	-18,33799934	1616940	0,00932212	-49,58840179	0,026298501	0,186139002	-0,006805	-0,025660001	0,065259904
25_1	-0,0080116	14,7354002	374,0899963	-33,89649963	1099920	0,00634002	-39,94860077	-0,00880432	0,186139002	0,012323	0,02809	0,074620001
50_1	-0,0088026	18,19239998	455,8500061	-34,93500137	1031000	0,00594312	-38,39070129	-0,0172043	0,186139002	0,014107	0,02554	0,074089997
75_1	-0,009233	20,1432991	439,3900146	-35,58760071	1117000	0,00643872	-40,32429886	-0,017601	0,186139002	0,014774	0,028580001	0,07401
100_1	-0,0094222	21,21199989	440,730011	-35,73839951	999600	0,00576032	-37,64640045	-0,023101799	0,186139002	0,014672	0,02747	0,074340001
1_1*	-0,0033227	3,67572999	330,2999878	-27,35440063	1531430	0,00883032	-48,21110153	0,0196991	0,186139002	0,00300002	0,0225699	0,06961
25_1*	-0,0079508	14,74069977	404,3399963	-33,86349869	1211410	0,00698372	-42,31909943	-0,00559998	0,186139002	0,013072	0,0276899	0,073810004
50_1*	-0,0086921	17,63540077	442,1900024	-34,34970093	1053750	0,00607302	-38,90909958	-0,0146027	0,186139002	0,013929	0,0242	0,073899999
75_1*	-0,0091351	19,92329979	454,3900146	-35,48690033	875620	0,00504392	-34,5530014	-0,024803201	0,186139002	0,015277	0,02369	0,0736899
100_1*	-0,0093655	20,55879974	476,4299927	-35,66270065	872230	0,00502422	-34,46409988	-0,025802599	0,186139002	0,015563	0,025399899	0,074989997
100_100	-0,0014422	3,137269974	371,0499878	-23,02129936	1459420	0,00841192	-46,98059845	0,017593401	0,186139002	-0,00114298	-0,017710101	0,067610003
100_25	-0,004687	7,240099907	407,6099854	-29,62269974	1359070	0,00783492	-45,18790054	0,00799561	0,186139002	0,00580806	0,00301993	0,072979897
100_50	-0,0031765	5,447800159	397,5299988	-27,73690033	1332700	0,00768032	-44,68759918	0,0114975	0,186139002	0,00295204	-0,0121801	0,072439998
100_75	-0,0022329	4,14289999	414,6799927	-26,03420067	1390970	0,00801772	-45,76850128	0,0147934	0,186139002	0,000755012	-0,0133301	0,073949903
25_100	0,000208801	1,277670026	354,5	-21,81809998	1629710	0,00939622	-49,78990173	0,024498001	0,186139002	-0,00431496	-0,022010099	0,06972
25_25	-0,0016015	2,866159916	385,6499939	-23,80940056	1672900	0,00964582	-50,4571991	0,0226974	0,186139002	-0,000390947	-0,00759006	0,070419997
25_50	-0,000671299	1,936400056	363,9299927	-23,54509926	1637400	0,00944122	-49,91149902	0,0233994	0,186139002	-0,00236499	-0,0142101	0,070819996
25_75	-0,000388199	1,849509954	326,5700073	-21,98870087	1378560	0,00794552	-45,54079819	0,020095799	0,186139002	-0,00284696	-0,016130099	0,062830001
50_100	-0,000334399	1,872249961	357,3200073	-22,79529953	1704980	0,00983012	-50,93889999	0,023696899	0,186139002	-0,00409698	-0,021740099	0,074320003
50_25	-0,0032721	4,83010006	436,3699951	-26,49920082	1346090	0,00775802	-44,94039917	0,0129929	0,186139002	0,00239003	-0,0010401	0,068400003
50_50	-0,0018542	3,108999968	369,6900024	-25,45560074	1509740	0,00870382	-47,84500122	0,0183945	0,186139002	0,000240028	-0,0105101	0,069750004
50_75	-0,0011289	2,790849924	379,6099854	-24,63129997	1367280	0,00788002	-45,33240128	0,0172958	0,186139002	-0,00156599	-0,01598	0,065959901
75_100	-0,0011868	2,969899893	359,8299866	-22,88969994	1503170	0,00866492	-47,73130035	0,0195999	0,186139002	-0,00210798	-0,0228101	0,063979998
75_25	-0,00403	6,079100132	425,8800049	-29,05170059	1260220	0,00726402	-43,29539871	0,00930023	0,186139002	0,00500304	-0,000880003	0,071759902
75_50	-0,0023129	4,016139984	363,75	-24,89520073	1308020	0,00753902	-44,22280121	0,0135956	0,186139002	0,00141603	-0,0112901	0,066699997
75_75	-0,0016406	3,663980007	384,2799988	-25,8906002	1508850	0,00869962	-47,83250046	0,017898601	0,186139002	-0,000639975	-0,02029	0,069049999
10_90	0,0008051	0,959659994	361,6300049	-20,49539948	1720510	0,00991982	-51,17010117	0,025993301	0,186139002	-0,00591195	-0,025739999	0,070160002
20_80	0,000187501	1,271780014	320,25	-20,06999969	1642440	0,00946942	-49,98749924	0,0246964	0,186139002	-0,00370997	-0,023070101	0,065499999
30_70	-0,0003931	1,901450038	381,5100098	-22,27389908	1454850	0,00838612	-46,90269852	0,020996099	0,186139002	-0,00331497	-0,018220101	0,06876
40_60	-0,000974499	2,542779922	377,7999878	-23,29640007	1411340	0,00813512	-46,1352005	0,0183945	0,186139002	-0,00241798	-0,0194501	0,069179997
60_40	-0,000974499	1629990	377,7999878	-23,29640007	5,97946E+11	664387008	-101,8280029	0,0183945	0,186139002	-0,00241798	-0,0194501	0,069179997
70_30	-0,000974499	1629990	377,7999878	-23,29640007	5,97946E+11	664387008	-101,8280029	0,0183945	0,186139002	-0,00241798	-0,0194501	0,069179997
80_20	-0,0047317	8,013999939	430,8800049	-30,80220032	1239460	0,00714362	-42,88010025	0,00499725	0,186139002	0,00542903	-0,00133002	0,069649898
90_10	-0,0067076	11,74230003	466,6199951	-32,98649979	1191800	0,00687052	-41,91529846	-0,00270081	0,186139002	0,010214	0,01289	0,072809897

SLEUTH	At1_Cl1	At2_Cl1	ANew_Cl1	AInf_Cl1	AEdg_Cl1	AOut_Cl1	MEI_Cl1	AWM_Cl1	CP_Cl1	RC_Cl1	Ac_Cl1	Ar_Cl1
1_1	68,84459686	88,13249969	19,28790092	3,528000116	13,28040028	2,47950006	34,38290024	33,40430069	11,14239979	0,493979007	19,28790092	0,385758013
1_25	68,84459686	88,27290344	19,42830086	6,600599766	11,78999996	1,03770006	40,46509933	44,35179901	11,22200012	0,497162998	19,42830086	0,388565987
1_50	68,84459686	88,11720276	19,27260017	6,039899826	12,37769985	0,85500002	41,66749954	44,98149872	11,13239956	0,493631989	19,27260017	0,385452002
1_75	68,84459686	87,54840088	18,7038002	6,242400169	11,5685997	0,89279997	41,43970108	45,57440186	10,80420017	0,480679989	18,7038002	0,374076009
1_100	68,84459686	87,39990234	18,55529976	5,610599995	12,23190022	0,71280003	42,39609909	45,68230057	10,71759987	0,477284998	18,55529976	0,371105999
25_1	68,84459686	88,18019867	19,3355999	1,758599997	10,41569996	7,16130018	22,5814991	20,76849937	11,17129993	0,49506101	19,3355999	0,386712015
50_1	68,84459686	88,17299652	19,32839966	1,58220005	9,673199654	8,07299995	20,38529968	18,91640091	11,16810036	0,494897991	19,32839966	0,38656801
75_1	68,84459686	88,18650055	19,34189987	1,541700006	9,179100037	8,62110043	19,15509987	18,10740089	11,17500019	0,495204002	19,34189987	0,386837989
100_1	68,84459686	87,9992981	19,15469933	1,559700012	8,528400421	9,06659985	18,61989975	17,46839905	11,06669998	0,490954012	19,15469933	0,383094013
1_1*	68,84459686	88,12619781	19,28160095	3,890700102	12,7656002	2,62529993	33,604599	33,07699966	11,13850021	0,493835986	19,28160095	0,385632008
25_1*	68,84459686	88,21440125	19,36980057	1,898100019	10,48050022	6,99119997	22,31559944	21,00530052	11,19079971	0,495837003	19,36980057	0,387396008
50_1*	68,84459686	88,15049744	19,30590057	1,664999962	9,644399643	7,99650002	20,43009949	19,3416996	11,15400028	0,494388014	19,30590057	0,386117995
75_1*	68,84459686	88,09919739	19,25460052	1,638900042	8,775899887	8,83979988	19,58749962	18,09959984	11,1243	0,493223011	19,25460052	0,38509199
100_1*	68,84459686	88,28639984	19,44179916	1,58039999	8,581500053	9,2798996	19,05719948	17,70669937	11,23250008	0,497469008	19,44179916	0,388835996
100_100	68,84459686	87,73470306	18,89010048	4,879799843	11,93939972	2,07089996	35,332901	40,34339905	10,91090012	0,484932005	18,89010048	0,377802014
100_25	68,84459686	88,5510025	19,70639992	3,47939992	12,03569984	4,19129992	29,32649994	31,76959991	11,38399982	0,50345403	19,70639992	0,394127995
100_50	68,84459686	88,53659821	19,69199944	4,536900043	11,79179955	3,36330009	31,51939964	35,78340149	11,37419987	0,503129005	19,69199944	0,393839985
100_75	68,84459686	89,44380188	20,5991993	5,453999996	12,28680038	2,85840011	33,00740051	38,38840103	11,8987999	0,523518026	20,5991993	0,411983997
25_100	68,84459686	88,61849976	19,77389908	6,263100147	12,13560009	1,37520003	39,17699814	43,73130035	11,42179966	0,504978001	19,77389908	0,39547801
25_25	68,84459686	88,39080048	19,5461998	4,887899876	12,53339958	2,1249001	35,73070145	39,20610046	11,29030037	0,499832004	19,5461998	0,390924007
25_50	68,84459686	88,51679993	19,67219925	5,138999939	12,93570042	1,59749997	37,63410187	41,49449921	11,36340046	0,502681017	19,67219925	0,393444002
25_75	68,84459686	86,58270264	17,73810005	5,185800076	11,09700012	1,45529997	38,02719879	42,88150024	10,24580002	0,458496988	17,73810005	0,354761988
50_100	68,84459686	89,53289795	20,68829918	5,923799992	13,04459953	1,71990001	37,38119888	42,47779846	11,94939995	0,525509	20,68829918	0,413765997
50_25	68,84459686	87,83640289	18,99180031	4,17509985	11,8125	3,00419998	32,29219818	35,29539871	10,9701004	0,487248987	18,99180031	0,379835993
50_50	68,84459686	88,20089722	19,35630035	4,932899952	12,06630039	2,35710001	35,12360001	38,82839966	11,18089962	0,495530993	19,35630035	0,387125999
50_75	68,84459686	87,48090363	18,63629913	5,128200054	11,54880047	1,95930004	36,21969986	41,02669907	10,76439953	0,479137987	18,63629913	0,372725993
75_100	68,84459686	86,98590088	18,1413002	4,853700161	11,23019981	2,05739999	36,07400131	41,07490158	10,47850037	0,467788994	18,1413002	0,36282599
75_25	68,84459686	88,22969818	19,38509941	3,59100008	12,01410007	3,77999997	30,62649918	33,2655983	11,19849968	0,496183991	19,38509941	0,387701988
75_50	68,84459686	87,18389893	18,33930016	4,588200092	11,08440018	2,66669989	33,79449844	38,06399918	10,59370041	0,472335994	18,33930016	0,366786003
75_75	68,84459686	88,21620178	19,3715992	5,133600235	11,82509995	2,41289997	34,26169968	40,17739868	11,19029999	0,495878011	19,3715992	0,387432009
10_90	68,84459686	88,76429749	19,91970062	7,026299953	11,86830044	1,02509999	39,7677002	45,41600037	11,5053997	0,508265972	19,91970062	0,398393989
20_80	68,84459686	87,34590149	18,50130081	5,975999832	11,24100018	1,28429997	39,43859863	43,85739899	10,6864996	0,476049006	18,50130081	0,370025992
30_70	68,84459686	88,20359802	19,35899925	5,785200119	11,92140007	1,65240002	37,77460098	42,64199829	11,18200016	0,495591998	19,35899925	0,387180001
40_60	68,84459686	88,18379974	19,33919907	5,468400002	12,02760029	1,84319997	36,44900131	40,98149872	11,17080021	0,495142996	19,33919907	0,386783987
60_40	68,84459686	88,5042038	19,6595993	4,604400158	12,1157999	2,93939996	33,06309891	37,14730072	11,35540009	0,502397001	19,6595993	0,393191993
70_30	68,84459686	87,79679871	18,95219994	4,184100151	11,33100033	3,43709993	30,97990036	34,63880157	10,94760036	0,48634699	18,95219994	0,379043996
80_20	68,84459686	87,97319794	19,12859917	3,715199947	10,93050003	4,48290014	28,80319977	31,73259926	11,05010033	0,490361005	19,12859917	0,382571995
90_10	68,84459686	88,21350098	19,3689003	2,774699926	10,49040031	6,10379982	25,20689964	25,94070053	11,19029999	0,495817006	19,3689003	0,387378007